Current Research in Toxicology 6 (2024) 100156

Contents lists available at ScienceDirect

Current Research in Toxicology

journal homepage: www.journals.elsevier.com/current-research-in-toxicology

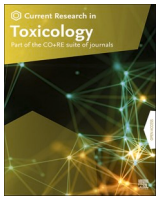

Investigating open access new approach methods (NAM) to assess biological points of departure: A case study with 4 neurotoxic pesticides

Marilyn H. Silva [1]

University of California, Davis, CA 95616, USA

ARTICLE INFO

Keywords:
New Approach Methods (NAM)
Integrated Chemical Environment (ICE)
Endosulfan
Fipronil
Propyzamide
Carbaryl
ToxCast
High Throughput Transcriptomics (HTTr)
High Throughput Phenotypic Profile (HTPP)

ABSTRACT

Open access new approach methods (NAM) in the US EPA ToxCast program and NTP Integrated Chemical Environment (ICE) were used to investigate activities of four neurotoxic pesticides: endosulfan, fipronil, propyzamide and carbaryl. Concordance of *in vivo* regulatory points of departure (POD) adjusted for interspecies extrapolation (AdjPOD) to modelled human Administered Equivalent Dose (AED_{Human}) was assessed using 3-compartment or Adult/Fetal PBTK *in vitro* to *in vivo* extrapolation. Model inputs were from Tier 1 (High throughput transcriptomics: HTTr, high throughput phenotypic profiling: HTPP) and Tier 2 (single target: ToxCast) assays. HTTr identified gene expression signatures associated with potential neurotoxicity for endosulfan, propyzamide and carbaryl in non-neuronal MCF-7 and HepaRG cells. The HTPP assay in U-2 OS cells detected potent effects on DNA endpoints for endosulfan and carbaryl, and mitochondria with fipronil (propyzamide was inactive). The most potent ToxCast assays were concordant with specific components of each chemical mode of action (MOA). Predictive adult IVIVE models produced fold differences (FD) < 10 between the AED_{Human} and the measured *in vivo* AdjPOD. The 3-compartment model was concordant (i.e., smallest FD) for endosulfan, fipronil and carbaryl, and PBTK was concordant for propyzamide. The most potent AED_{Human} predictions for each chemical showed HTTr, HTPP and ToxCast were mainly concordant with *in vivo* AdjPODs but assays were less concordant with MOAs. This was likely due to the cell types used for testing and/or lack of metabolic capabilities and pathways available *in vivo*. The Fetal PBTK model had larger FDs than adult models and was less predictive overall.

1. Introduction

New approach methods (NAMs) are an ever-expanding range of methods with potential for use in chemical risk assessment that include, for example, quantitative structure–activity relationship predictions (QSAR), *in silico* (e.g., high-throughput toxicokinetics: httk), high-throughput screening bioassays, advanced imaging/scanning techniques, computational modeling (*in vitro* to *in vivo* extrapolation: IVIVE), omics applications (e.g., transcriptomics, genomics), cell and organoid cultures, microphysiological systems, machine learning models, artificial intelligence and other methods currently in development (Schmeisser et al., 2023). NAMs generally do not use intact animals (*in vivo*), but employ technologies, methodologies, or combinations of approaches to provide information on chemical hazard identification (US EPA, 2018). NAMs are becoming more accessible to regulatory agencies and researchers for pesticide screening, prioritization and risk assessment through the United States Environmental Protection Agency Office of Research and Development (US EPA/ORD) CompTox Chemicals

Abbreviations: AC_{50}, Activity at 50% concentration; AChE, acetylcholinesterase; Adj, Adjusted interspecies extrapolation for BMDs and LOELs; AED_{human}, administered equivalent doses in humans; BMD, Benchmark Dose; BMR, Benchmark Response; BPAC, biological pathway altering concentration; CARB, carbaryl; CDPR, California Department of Pesticide Regulation; CNS, central nervous system; 3COMP, three compartment ICE model; CompTox, computational toxicology; DNT, developmental neurotoxicity; ENDO, endosulfan; FIP, fipronil; GABAa, γ-amino-butyric acid (GABA)-alpha; hNPC5, human neural progenitor cell line; HTPP, high throughput phenotypic profiling; httk, high throughput toxicokinetics; HTTr, high throughput transcriptomics; ICE, integrated chemical environment; IVIVE, *in vitro* to *in vivo* extrapolation; LOEL, lowest observed effect level; MAD, median absolute deviation; MOA, mode of action; NAM, new approach methods; PAC, phenotype altering concentration; PBTK, physiologically based toxicokinetic ICE model; POD, point of departure; PRZ, propyzamide; tcpl, ToxCast Pipeline; ToxCast, US EPA Toxicology Forecaster program; TK, toxicokinetic; US EPA, United States Environmental Protection Agency.

E-mail addresses: marilynhelensilva@gmail.com, mhsilva@ucdavis.edu.

[1] Retired from a career in toxicology and risk assessment, California Environmental Protection Agency; current Co-Chair Community Stakeholders' Advisory Committee, University of California, Davis, CA, 95616, USA.

https://doi.org/10.1016/j.crtox.2024.100156
Received 14 August 2023; Received in revised form 28 December 2023; Accepted 9 February 2024
Available online 15 February 2024
2666-027X/© 2024 The Author(s). Published by Elsevier B.V. This is an open access article under the CC BY-NC-ND license (http://creativecommons.org/licenses/by-nc-nd/4.0/).

Dashboard (CompTox Chemicals Dashboard (epa.gov)) that includes the Toxicity Forecaster (ToxCast) database (CompTox Chemicals Dashboard Assay Lists (epa.gov)). The National Toxicology Program (NTP) Integrated Chemical Environment (ICE) (Integrated Chemical Environment (ICE) (nih.gov)) includes the Tox21 database. Together ToxCast/Tox21 have over 1,400 assays and activity data for more than 9,000 chemicals, in addition to numerous computational toxicology tools, such as *in vitro* to *in vivo* extrapolation (IVIVE) models (Abedini et al., 2021; Bell et al., 2020; Hines et al., 2022; Jeong et al., 2022). NAMs development speeds hazard characterization of untold numbers of environmental chemicals to help close the current gaps in information on exposure, hazard identification and health risk that prevent timely regulatory decision-making (Woodruff et al., 2023). The US EPA and NTP CompTox databases and ongoing research are designed to aid in closing these knowledge gaps. According to Buckley et al. (2023) the three strategic program aspects involve chemical curation, data development and modeling as well as use of the FAIR principles: Findability, Accessibility, Interoperability, and Reuse of digital assets (Wilkinson et al., 2016). Open access data availability, transparency and work-flow examples facilitate NAMs use in risk assessment and other regulatory decisions (Buckley et al., 2023).

Pesticide registration in the United States requires testing in a battery of traditional bioassays, including *in vivo* dose–response animal studies to identify effects that could be hazardous to human health (US EPA, 1998). The purpose is to identify effects that may pose a risk, even if the effects in animals aren't necessarily exact predictions of what would occur in humans (Li et al., 2019; Shanks et al., 2009). However, the traditional *in vivo* tests for pesticide registration generally lack mechanistic data, they are costly, and time consuming and animal studies involve ethical and relevance issues as well (Hansen & Kosberg, 2019). Moreover, the US EPA is charged with eventually eliminating mammalian study requests by 2035 (Thomas et al., 2019). Hence, research and regulatory agencies have developed NAMs to supplement, support and/or replace *in vivo* bioassays submitted for regulatory actions (Abedini et al., 2021; Bell et al., 2020; Carstens et al., 2022; Chang et al., 2022; Knudsen et al., 2021; Punt et al., 2020; Richard et al., 2020; Williams et al., 2017).

NAMs are used to investigate xenobiotic chemical targets potentially involved in molecular initiating events, modes of action (MOA) or adverse outcome pathways (AOP) leading to pesticidal *in vivo* apical endpoints. Data are gathered, integrated, and evaluated using computerized mathematical methods to predict points of departure (POD) from *in vitro* assays generated through a series of increasingly refined open access CompTox tools. On the CompTox Chemicals Dashboard the available ToxCast databases have hundreds of targeted cell-based and cell free assays mainly designed to test a single compound at a time. Moving forward, new assay methods for hazard identification such as high throughput transcriptomics (HTTr) and high throughput phenotypic profiling (HTPP) have been developed to improve efficiency in testing and increase biological coverage through broad based non-targeted assays (Harrill et al., 2021; Nyffeler et al., 2023). HTTr and HTPP can provide insights into how a chemical affects a whole cell by identifying gene expression as well as phenotypic changes from exposure. Hence, the focus is on a transcriptomic gene expression signature or a phenotypic endpoint that can provide a foundation of knowledge to be followed by examination of ToxCast targeted assays. Together the HTTr, HTPP and ToxCast assays can be used for mechanistic insights and potency estimations, as well as screening and prioritization.

The HTTr signatures, HTPP and ToxCast *in vitro* data can input into ICE-modeled *in vitro* to *in vivo* extrapolation (IVIVE) with the 3 compartment (3COMP), the physiologically based toxicokinetic (PBTK) adult and Fetal PBTK models to generate administered equivalent doses (AED_{Human}: mg/kg) for comparison with measured *in vivo* PODs (Abedini et al., 2021; Bell et al., 2020; Hines et al., 2022). These comparisons can then provide insights into the potential usefulness of the NAMs for chemical screening, ranking and hazard characterization. Further, where it was previously necessary to understand certain coding methods to model data, the ICE models used in this study are open access and do not require knowledge of coding. On the other hand, codes are also available through links published on the ICE website.

This case study investigates activities of four neurotoxic pesticides of two different classifications (insecticide and herbicide) that are currently being used in the United States and/or internationally (Fig. 1). Each has been characterized through comprehensive risk assessments by the US EPA or state agencies. Endosulfan (ENDO: CAS 115–29-2 [6,7,8,9,10,10-Hexachloro-1,5,5a,6,9,9a-hexahydro-3H-6,9-methano-3λ ~ 4 ~ -2,4,3λ ~ 4 ~ -benzodioxathiepin-3-one]) (CDPR, 2008) is an organochlorine insecticide and fipronil (FIP: CAS 120068–37-3 [5-amino-1-[2,6-dichloro-4-(trifluoromethyl)phenyl]-4-[(trifluoromethyl) sulfinyl]-1Hpyrazole-3-carbonitrile]) (CDPR, 2023) is a phenylpyrazole insecticide. Both pesticides block chloride ion channels on the ϒ-aminobutyric acid alpha receptor (GABAaR). Propyzamide (PRZ: CAS 23950–58-5; 3,5-Dichloro-N-(2-methylbut-3-yn-2-yl) benzamide) is a benzamide herbicide, that is known to induce cytochrome P450s (CYP), leading to oxidative stress, however, acute effects are neurotoxic based on the increase in landing foot splay in female rats and the decrease in motor activity seen in male rats on Day 1 of treatment (US EPA, 2015). Carbaryl (CARB: 63–25-2; Naphthalen-1-yl methylcarbamate) (US EPA, 2017) is a carbamate insecticide that acts by inhibition of acetylcholine esterase (AChE). The pesticides were examined in Tier 1 HTTr, and in the HTPP assay, as well as Tier 2 ToxCast assays to see what targets are identified in the known pathways of these well-characterized chemicals. Then the HTTr biological pathway altering concentrations (BPACs) and HTPP phenotype altering concentrations (PACs) for the Tier 1 assays (reported as Benchmark Dose [BMD], μM) and the activity at 50 % concentration (AC_{50} μM) for the Tier 2 assays are entered into the ICE 3COMP, PBTK and Fetal PBTK IVIVE models to predict PODs (mg/kg/day). Subsequently they are compared to regulatory PODs based on animal models. Further, the potency for each test method was determined and concordance between the most potent BMD and AC_{50} and the known MOA were reported.Fig. 2..

2. Methods

2.1. Pesticide points of departure for Endosulfan, Fipronil, Propyzamide and Carbaryl

The *in vivo* PODs for each pesticide were selected from regulatory, open access documents that are used for pesticide regulation (CDPR, 2008, 2023; US EPA, 2015, 2017). The POD for ENDO was based on neurotoxic effects (e.g., tremors, convulsions) in pregnant rabbits and a Lowest Observed Effect Level was determined (LOEL; CDPR (2008)). The POD for FIP was for a neurotoxic effect (increased hindlimb splay) in rats determined by Benchmark Dose (BMD) analysis with a Benchmark Response of 10 % (BMD_{10}) (CDPR (2023)). The POD for PRZ was for acute decreases in motor activity and landing foot-splay in rats based

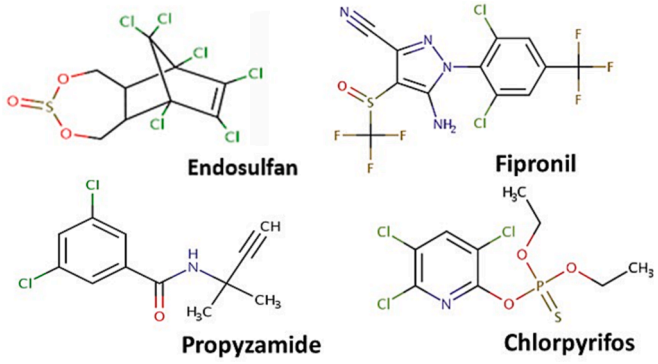

Fig. 1. Structures of the neurotoxic pesticides examined in this study.

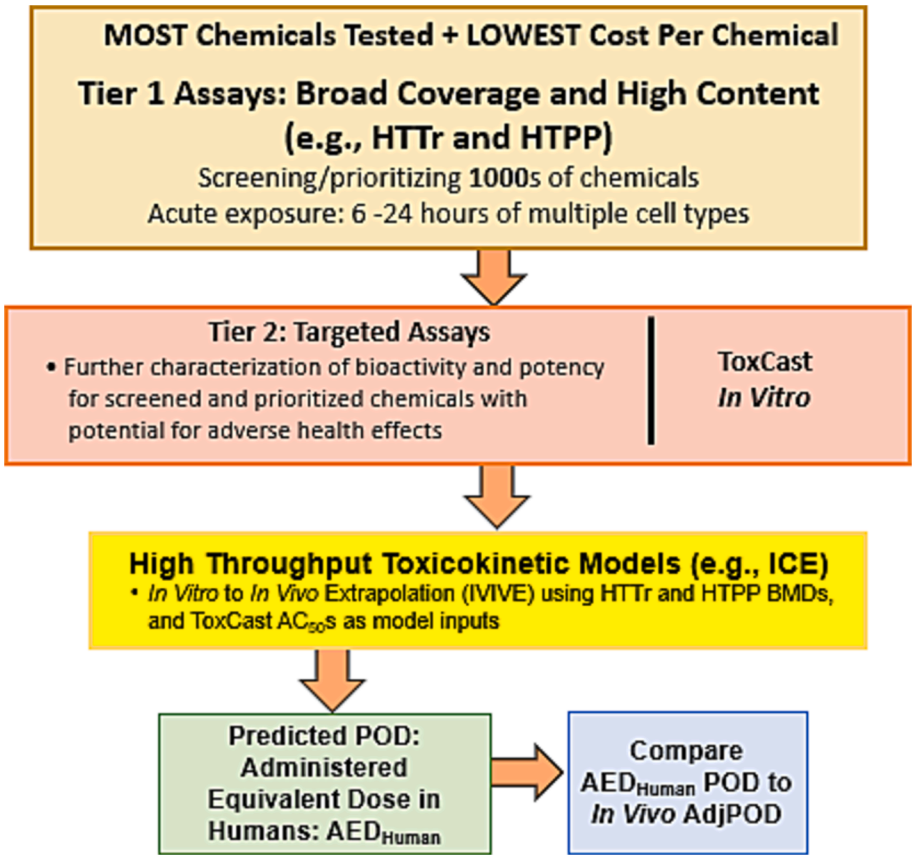

Fig. 2. A tiered approach encompassing New Approach Methodologies (NAM) is described for screening, prioritizing and chemical characterization. Tier 1 involves knowledge of chemical structure, along with use of assays with broad coverage, high content, and multiple cell types. Chemicals with predictions of biological targets or pathways from Tier 1 can be further characterized in Tier 2 by use of *in vitro* targeted assays (e.g., ToxCast). Tier 1 High throughput transcriptomics (HTTr) gene expression signature and high throughput phenotypic profile endpoint (HTPP) benchmark doses (BMD μM) and Tier 2 ToxCast AC_{50}s (μM) can be used in various Integrated Chemical Environment Tools such as *in vitro* to *in vivo* extrapolation (IVIVE) models to produce human administered equivalent doses (AED_{Human} mg/kg) as points of departure (POD). Predicted PODs can be compared to regulatory *in vivo* PODs after applying an interspecies (animal to human) 10-fold extrapolation *(in vivo* AdjPOD), to assess concordance.

on a LOEL (US EPA (2015). The POD for CARB was for acetylcholinesterase inhibition (AChE) in the brain determined by BMD analysis with a Benchmark Response of 10 % (BMD_{10}) in rats (US EPA (2017), Table 1).

LOEL/BMD_{10} values were used in this study as a point of departure because they are the lowest measured level of biological activity that is comparable to the HTTr BMD/Biological Pathway Altering Concentration (BPAC), HTPP BMD (PAC) and ToxCast AC_{50} (Harrill et al., 2021; Judson et al., 2014; Sipes et al., 2011b). ToxCast *in vitro* data were reported as an AC_{50} (μM), comparable to a LOEL or BMD, as has been shown previously (Paul Friedman et al., 2020; Sipes et al., 2011a). The AC_{50} values for the ToxCast assays were preferred as an *in vitro* POD because it provided the greatest confidence in the range where the true activity lies (Watt & Judson, 2018). That is, values at the lowest end of the dose–response curve may be less certain due to decreased efficacy and significance, as well as an increase in noisy data (Filer et al., 2017). Since the BMD_{10} and LOEL derived studies were performed in animals, a default uncertainty factor of 10 was added to adjust for interspecies extrapolation for differences in toxicokinetic parameters between

Table 1
Acute *In Vivo* regulatory endpoints for endosulfan, fipronil, propyzamide and carbaryl.

Animal Strain	Treatment	Doses mg/kg	Acute Effect	POD mg/kg/day	AdjBMD_{10}/LOEL[a] mg/kg/day	Ref[b]
Endosulfan: Developmental Rabbit						
Pregnant New Zealand White	Gavage GD 6–28	0 (corn oil), 0.3, 0.7, 1.8	Neurotoxicity signs from treatment day one	LOEL 1.8	AdjLOEL 0.18	1
Fipronil: Acute Rat						
Adult: Crl:CD BR	Gavage, single	0 (corn oil), 2.5, 7.5, 25	↑Hindlimb splay	BMD_{10} 2.5	AdjBMD_{10} 0.25	2
Propyzamide: Neurotoxicity Rat						
Adult: F344/DuCrl	Gavage, single	0 (corn oil), 40, 200, 600	↓ Motor activity (♂) ↑ Landing foot-splay (♀)	LOEL 40	AdjLOEL 4.0	3
Carbaryl: Acute Rat						
Pup: Male Long-Evans	Gavage, single PND 11	0 (corn oil), 3, 7.5, 15, 30	↓Brain AChE	BMD_{10} 1.46	AdjBMD_{10} 0.146	4

Abbreviations: Adj: adjusted; BMD_{10}: Benchmark Dose (10% benchmark response); GD: Gestation Day; LOEL: Lowest-observed-effect-level; PND: Postnatal Day.
[a] - Lowest effect levels (BMD_{10}/LOEL) were divided by a default interspecies factor of 10 to account for animal to human (interspecies) variability.
[b] -1. CDPR (2008), 2. CDPR (2023), 3. US EPA (2015), 4.US EPA (2017).

animal and human (AdjPOD) (US EPA, 2002b; WHO, 2014, 2017). Interspecies adjustments were made because most of the *in vitro* assays were performed with cultured human cells and because the ICE IVIVE models were designed using human pharmacokinetic parameters when possible.

2.2. Tiered in vitro New approach methodologies

The future of computational toxicology for hazard identification, risk assessment and other chemical characterization has been represented as a Tiered approach (Fig. 1) (Thomas et al., 2019).

Tier 1 is comprised, in part, of acute (6–24 h) non-targeted assays with broad biological target coverage and high content readouts that can be performed in a variety of cell types (Thomas et al., 2019). Tier 1 methods that can increase the efficiency of detecting chemical bioactivity at molecular targets include: 1) HTTr where transcripts are measured in response to chemical treatment in various cultures of human cell lines (e.g. MCF7, U-2 OS and HepaRG) followed by concentration–response analysis of gene expression signature scores (Harrill et al., 2021). The assays produce transcriptional BPACs that potentially align with ToxCast *in vitro* assays available on the CompTox Chemicals Dashboard and identify gene expression signatures associated with molecular targets. The most potent and efficacious BPACs can correspond to known mechanisms for tested chemicals; 2) HTPP methodologies where similar or the same cultured human cell lines are fluorescently labeled to produce images of subcellular structures as well as quantify cellular morphological changes as a result of chemical treatment (Nyffeler et al., 2023). The version of the CompTox Chemicals Dashboard (version 2.2.1) used in this study reported HTPP assay results in U-2 OS cells. HTPP methods result in quantifiable and reproducible visible changes in cell morphology.

Tier 2 can involve targeted *in vitro* ToxCast assays as are found on the CompTox Chemicals Dashboard (CompTox Chemicals Dashboard (epa.gov)). Targeted assays are performed using cell, or cell-free methods and are designed to help characterize bioactivity and chemical potency and identify potential AOPs or MOAs. This tier follows from the compilation and analysis of Tier 1 data ("orthogonal confirmation": Thomas et al. (2019)).

Note that while HTTr assays reported on the CompTox Chemicals Dashboard (v2.2.1; accessed 10–2023; CompTox Chemicals Dashboard (epa.gov)) were performed with MCF-7, U-2 OS and HepaRG cells, where the HTPP assay reportedly used only U-2 OS. While the cell types used in Tier 1 are not neuronal cells, and the four pesticides are neurotoxic, the methods are designed to detect generalizable and broadly applicable activities that can be applied to detection of many potent biological perturbations (BPAC/PAC) through effects on gene expression or changes in cell morphology (Bray et al., 2016; Harrill et al., 2021). In addition, the CompTox Chemicals Dashboard is often updated to include more assays and high throughput methods.

HTTr, HTPP and ToxCast assays from both Tiers were used in high throughput toxicokinetic models (e.g., ICE) IVIVE to generate AED_{Human} PODs to compare to *in vivo* Regulatory PODs. Chemical potency and concordance with *in vivo* AdjPODs and mechanistic pathways are also described.

2.3. High throughput Transcriptomics, high throughput phenotypic profiling endpoints and ToxCast in vitro data

2.3.1. High throughput transcriptomics (HTTr)

Tier 1 HTTr is a process used to profile gene mRNA levels expressed after chemical treatment in different human cell lines (e.g., MCF-7, U-2 OS, HepaRG) (Harrill et al., 2019; Harrill et al., 2021). Use of diverse cell types can facilitate detection of a wide variety of gene expression changes. For example, molecular targets expressed in the MCF-7 human cell line include estrogen receptor alpha (ESR1), androgen receptor (AR), peroxisome proliferator activating receptor alpha and gamma (PPARα and PPARϒ, respectively), 3-hydroxy-3-methylglutaryl-CoA reductase (HMGCR), and thyroid hormone receptor alpha (THRα) (Harrill et al., 2021).

Data were obtained from Templated Oligo with Sequencing Readout (TempO-Seq) whole transcriptome assay (Harrill et al., 2021). Gene expression fold-change profiles for each treatment were modeled to obtain signature enrichment scores based on the fold changes of genes within a signature versus genes not included in the signature. Test chemicals and gene expression signature scores were then analyzed by tcplfit2 (R-Package available for download: CRAN - Package tcplfit2 (r-project.org). Continuous hit-calls, calculated by criteria provided within the tcplfit2 R-package have a value between zero and one, with values closer to one indicating a higher likelihood of a biological response (i.e. hit) (Sheffield et al., 2021). Continuous hit-calls of signature-level enrichment scores identified molecular targets associated with the transcriptional bioactivity (Sheffield et al., 2021). Hit-call values at 0.9 and greater were acceptable for this study since the higher values indicate greater confidence in classifying a modeled endpoint as a hit.

Potency is an estimate of the BPAC where the winning model curve crosses the benchmark response (BMR = [1.349] x [signature-specific noise level]) (Filipsson et al., 2003; Thomas et al., 2007; Yang et al., 2007). BMD upper and lower bounds were calculated by the profile likelihood method (Banga et al., 2002). In Supplemental Tables 1-4 there are columns entitled "QC Flag" with no data listed. However, QC metrics used for processing and analyzing HTTr data were detailed in Harrill et al. (2021) and included, among others, filtering out cytotoxic treatments that "no longer represent molecular initiating events".

2.3.2. High throughput phenotypic profiling (HTPP)

Tier 1 HTPP is a method of measuring phenotypic changes in cells (e.g., U-2 OS cell lines) by labeling a variety of organelles with fluoroprobes (Gustafsdottir et al., 2013; Nyffeler et al., 2020). Data are produced as cellular images where morphological (e.g., structure or form) changes can occur after chemical exposures. HTPP fluorescent cytochemistry and high-content imaging identify changes in organelles (e.g., nucleus, nucleoli, endoplasmic reticulum [ER], golgi apparatus [G], mitochondria [Mito], actin cytoskeleton [A], plasma membrane [P]) and/or cellular shape to characterize dose–response effects. There are 1350 endpoints that can be analyzed in HTPP. This collection of endpoints is composed of 1300 phenotypic features, 49 feature categories, and 1 global endpoint (Nyffeler et al., 2023; Nyffeler et al., 2020). A category (channel_module_compartment) consists of a collection of features, or channels (e.g., DNA, RNA, ER, AGP, Mito), modules (e.g., feature types including intensity, texture, localization of fluorescent signal, shape and position of the cells) and compartments (cell compartment or organelle) (Nyffeler et al., 2020). As an example, one of the 49 categories is reported as "DNA_compactness_nuclei", indicating DNA "channel", compactness feature "module" and nuclei "compartment".

The global and category-level Mahalnobis distance metrics are subject to concentration–response modeling using the tcplfit2 R-package (version 0.1.0) (Sheffield et al., 2021). Mahalanobis distance data utilized nine BMD models (Poly1, Poly2, Power, Hill, Exp2-Exp5, constant: Benchmark Response = 1) to determine a BMD (μM) for each category (Nyffeler et al., 2021; Nyffeler et al., 2023). Curves with a hit-call probability of ≥ 0.9 were those considered active and a chemical was considered "phenotypically active" when a BMD could be established by a "Global Mahalanobis" approach or in a category by use of the "Category-level Mahalanobis" (Nyffeler et al., 2023). The category-level curve fitting Mahalanobis distance metrics is more applicable for POD determination because it is shown to have higher sensiti vity and lower risk for high-potency false positives when compared to the feature fitting approach (Nyffeler et al., 2021; Nyffeler et al., 2023). HTPP data selected for further analysis were determined as follows: 1) Initially data were sorted for hit-calls at > 0.9; 2) data were sorted for categories with

BMD concentrations at the global level or below and 3) a PAC defined as "…median potency of the most sensitive (i.e., potent) category, depending which value is lower" was determined (Nyffeler et al., 2020). The POD is synonymous with the PAC for category level fitting. An HTPP endpoint is described as a compilation of morphological features or latent variables that are subject to concentration–response modeling to determine if they are altered as a function of dose, 4) final data selections for this study were then based on most potent BMD.

In Supplemental Tables 1-4 there are columns entitled "QC Flag" with no data listed. However, QC metrics for processing and analyzing HTPP data include filtering out of cytotoxic treatments in the burst region prior to the concentration–response modeling (Nyffeler et al., 2023). It was noted in Nyffeler et al. (2021) that prior to BMD modeling of HTPP data, highly cytotoxic treatments were removed by excluding all tested concentrations above the cell viability lowest effective concentration (CV.LOEC).

2.3.3. ToxCast assay Criteria

ToxCast results downloaded from the open access: CompTox Chemicals Dashboard (epa.gov) (version 2.2.1, May 2023) (Supplemental Table 1) were examined for active hit-calls. ToxCast data were comprised of high throughput *in vitro* and *in vivo* (zebrafish) assays from numerous vendors and platforms (US EPA, 2023; Williams et al., 2017). Assays were performed with a variety of cells, including rat cortical neurons (primary brain cells), human cells (embryonic stem cells [hESC H9], embryonic kidney cell line [HEK293T], primary neural progenitor cells [hNPC], liver [primary; HepG2: hepatocyte carcinoma cell line; HepaRG: bi-potential hepatoma-derived cell line], and ovarian cell line [VM7]). Cell free (NVS: Novascreen) assays used human CYP1A1, CYP2C19, CYP2C9, CYP2J2 and rat CYP2A1 enzymes and cell-free deiodinase type 3 (DIO3) enzymes described on the CompTox Chemicals Dashboard for each chemical. Biological molecular targets were evaluated using ToxCast assays with data analyzed by concentration–response modeling resulting in one or a series of AC_{50}s (Judson et al., 2011). The data downloaded from the CompTox Chemicals Dashboard had been filtered through the ToxCast Pipeline (tcpl) to evaluate curve fits and AC_{50} levels for quantitative evaluation (Filer, 2019; Filer et al., 2017). Final selection of active hit-calls associated with AC_{50}s was facilitated by the presence or absence of flags (tcpl level 6), in addition to quantitative uncertainty evaluations related to curve-fitting at tcpl level 7 (Williams et al., 2017). Flags related to curve-fits were generally: "Borderline active", "Only highest conc above baseline, active", "Less than 50 % efficacy", "Hit-call potentially confounded by overfitting", "Noisy data" (Supplemental Tables 1-4) (Filer, 2019; Filer et al., 2017). Assays with more than two flags were excluded from further analysis in this study because reproducible curve-fitting decreases with greater than or equal to three flags (Paul Friedman et al., 2020). Assays filtered and selected for further analysis in this study were either directly or peripherally associated with the MOA/AOP. Peripheral associations can include activity with nuclear receptors, or CYPs that are known to be involved with metabolic activation, or targets associated with chemical Phase II metabolism (e.g., glutathione transferase or sulfotransferase). *In vivo* zebrafish assays were excluded because for the four chemicals of interest neurotoxicity was not targeted.

Further selection occurred for hit-calls below the cytotoxicity lower limit for each chemical (data provided on the CompTox Chemicals Dashboard (epa.gov) and in Table 2). This value is greater than or equal to three median absolute deviations (MAD) below the median cytotoxicity limit (Judson et al., 2016). Assays at or below the cytotoxicity lower limit are more likely to represent true active hit-calls, as they are outside the burst region.

2.4. Z-score Calculations

After sorting the *in vitro* ToxCast assays of interest, a Z-Score was calculated to examine the likeliness that an active hit-call is associated with a specific chemical-target interaction that the assay is designed to assess (Judson et al., 2016). The cytotoxicity median and three MAD below the median (cytotoxicity lower limit) were reported for each chemical (Judson et al., 2016). A Z-Score of 3 or greater is an indication of chemical-target specificity for a given assay and the result is likely an active-hit-call below the range of cytotoxicity or cell stress (Paul Friedman et al., 2016; Zhang et al., 1999). Included in the Z-Score calculation is a "global cytotoxicity MAD" which is the median of the median absolute deviation of the $logAC_{50}$ based on ***cytotoxicity distributions across all chemicals*** (Judson et al., 2016; Kleinstreuer et al., 2017). Hence there is a cytotoxicity MAD on a per chemical basis and a global cytotoxicity MAD across all chemicals. The values are used to calculate the Z-Scores as shown in Equation 1:

$$\mathrm{Z-Score\,(chem,\,assay)} = ([-\mathrm{logAC50\,(chem,\,assay)}] - \mathrm{median}[-\mathrm{logAC50\,(chem,\,cytotox)}])/\mathrm{Global\,Cytotox\,MAD} \quad (1)$$

- 'chem, assay': Chemical and assay of interest
- -$logAC_{50}$ (chem, assay): Negative log of an AC_{50} for a chemical in an assay of interest.
- '-$logAC_{50}$' for the chemical and assay of interest
- '-$logAC_{50}$' for the chemical-specific median cytotoxicity limit
- -$logAC_{50}$ (chem, cyto): Negative log of the AC_{50} for a chemical-associated median cytotoxicity limit.
- 'Global Cytotox MAD': 'median of the median $logAC_{50}$ cytotoxicity assay distributions across all chemicals' = 0.29 log units (Judson et al., 2016)

Z-Score calculations were performed in Excel (Windows 11 v. 22H2) with values rounded to the nearest whole number (Supplemental Table 2).

2.5. Integrated chemical Environment (ICE) models 3COMP, PBTK and Fetal models

The ICE 3COMP, PBTK and Fetal PBTK oral models incorporate the US EPA httk R package, bioactivity (ToxCast AC_{50}s μM), physicochemical and chemical-specific toxicokinetic (TK) characteristics (e.g., metabolic properties) and reverse dosimetry parameters to predict *in vivo* exposures (AED_{Human} mg/kg/day) (ICE: https://ice.ntp.niehs.nih.gov/; version 4.0; updated 3/2023; Hines et al. (2022); Unnikrishnan et al. (2023); Abedini et al. (2021); Bell et al. (2020); Kapraun et al. (2022)). The oral route is the most likely means of exposure based on the pesticide use on crops. The models represent adult or fetal parameters that are not specific to sex. The "default" values option on the ICE dashboard was selected for absorption, distribution, metabolism, and elimination (ADME) parameter inputs. This option uses experimentally measured values when available, and *in silico* predictions when measured data were not available.

The 3COMP oral model used adult TK parameters. It has perfusion-limited compartments (i.e., equilibrium is achieved rapidly for tissue, RBC and plasma compared to flow of blood) comprised of gut, liver, and rest-of-body (e.g., fat, brain, bones). The "Solve_3comp" model from the open access ICE tool calculates plasma concentration over time. Hepatic metabolism and passive glomerular filtration of chemicals is the assumed form of elimination (Breen et al., 2021; Hines et al., 2022; Pearce et al., 2017) (ICE Tools (nih.gov)).

The "Solve_pbtk" model used adult TK parameters in a multi-compartment (gut, artery, vein, lung, liver, kidney, rest-of-body) function in the open access ICE tool. C_{max} is calculated for oral exposure at the 50th percentile using the average values for the PBTK parameters over time. Each compartment is perfusion-limited and has mass balance differential equations describing rate of change for quantity of chemical (Breen et al., 2021; Hines et al., 2022; Pearce et al., 2017) (ICE Tools

(nih.gov); calculations in Supplemental Table 4). The PBTK model was updated to incorporate US EPA's httk R package (version 2.2.2: released February 2023).

The human gestational, or Fetal PBTK model incorporates both maternal and fetal parameters from *in vitro* chemical measurements (Kapraun et al., 2022). Physiological parameter changes for mother and fetus during gestation days 91 to 280 were modeled. Data used in the model represented primarily healthy, low-risk Caucasian women with a single fetus, and an uncomplicated pregnancy. The gestational age was assumed to be the fetal age plus two weeks. **MATERNAL** changes measured included: 1) body weight, 2) plasma volume, 3) placenta volume, 4) adipose tissue mass, 5) cardiac output, 6) kidney blood flow, 7) glomerular filtration rate and 8) placental blood flow. **FETAL** changes measured included: 1) fetal volume, 2) liver mass, 3) kidney mass, 4) amniotic fluid volume, 5) blood flow through the placenta and 6) blood flow through the ductus arteriosus (Kapraun et al., 2019). Parameter changes not included: 1) maternal metabolic enzyme expression and activity, 2) fetal metabolic enzyme expression and activity, 3) fetal renal clearance capacities over development, and 4) maternal and fetal plasma protein binding (Kapraun et al., 2022). The Solve_fetal_pbtk utilizes the httk R package (version 2.2.2) to capture chemical distribution following an oral exposure as a function to solve for maternal and fetal compartment concentrations over time. Each tissue compartment is perfusion rate-limited, with the rate of change chemical concentration per tissue compartment described by mass balance differential equations. Chemical elimination is assumed to be by hepatic metabolism and passive glomerular filtration.

Reverse dosimetry calculations for acute oral exposures for humans were performed with an open access tool available on the ICE dashboard. Inputs into the models were BMDs from HTTr signatures and HTPP data (μM) and AC_{50}s (μM) from ToxCast. Outputs were AED_{Human} (mg/kg/day) that were subsequently compared to *in vivo* AdjLOEL/AdjBMD (mg/kg/day).

The fold-differences (FD) were determined between 3COMP or PBTK (adult or fetal) AED_{Human} (mg/kg/day) and regulatory AdjPODs. A 10-fold-difference between modelled and *in vivo* data is an acceptable range allowing for 3X for intraspecies variation due to TK differences among humans and 3X due to model uncertainty (total $\simeq$ 10) as the 3COMP, PBTK and Fetal PBTK models assume that ADME involves only a specific set of compartments (Dourson et al., 1996). FD predictions were considered to have "high concordance" if ≤ 5, be "concordant" if $> 5 < 10$ or have "low concordance" if > 10.

3. Results

3.1. In vivo points of departure

Regulatory LOELs and BMDs were available from open access reports for each chemical and were not determined by the author of this study: ENDO CDPR (2008); FIP CDPR (2023); PRZ US EPA (2015) and CARB US EPA (2017). A BMD at the 10 % response level (BMD_{10}) is a statistical calculation of a LOEL performed by CDPR and US EPA to obtain toxicological endpoints for FIP and CARB for single effect dose-responses (Table 1). ENDO and PRZ LOELs were determined from a range of neurotoxic effects. Interspecies default 10-fold uncertainty factors were applied to each chemical LOEL/BMD to produce AdjPODs and subsequent comparisons of ENDO and PRZ with their respective AED_{Human} values, shown below, are based on their comprehensive AdjLOEL effects.

3.1.1. Endosulfan (ENDO)

ENDO functions acutely as a non-competitive inhibitor in the central nervous system (CNS) by binding to specific subunits on the GABAa receptor subunit b3 that results in blockage of Cl- channels (Abalis et al., 1986; Casida, 1993; Ffrench-Constant et al., 2000; Lawrence & Casida, 1984; Ratra et al., 2001; Sutherland et al., 2004). GABAa receptors are the principal inhibitory neuroreceptors in the mammalian brain and antagonism of GABAergic neurons in the CNS causes generalized brain stimulation (Abalis et al., 1986; Cole & Casida, 1986; Gant et al., 1987; Ozoe & Matsumura, 1986) or uncontrolled excitation (Kamijima & Casida, 2000; Ratra et al., 2001). This effect is observed acutely in both humans and animals, where clinical signs were recorded. The acute LOEL for ENDO is 1.8 mg/kg/day from a developmental toxicity study in rabbits described in the Risk Characterization Document (CDPR, 2008) and the Risk Eligibility Decision (RED) (US EPA, 2002a). Although a developmental study in pregnant rabbits involves 22 days of gavage dosing, neurotoxic effects (hyperactivity) were observed within the first few days of treatment and that is why this study was selected for the acute oral LOEL (Table 1). The regulatory LOEL was adjusted 10-fold to extrapolate from rabbit to human (AdjLOEL = 0.18 mg/kg/day).

3.1.2. Fipronil (FIP)

Electrophysiological and ligand binding studies confirm that FIP reversibly and noncompetitively blocks passage of chloride ions through GABAa b3 receptors in the CNS (Ffrench-Constant et al., 1991; Ffrench-Constant et al., 1993; Mohamed et al., 2004). Humans exposed to FIP show symptoms such as headache, nausea, and seizures, which are associated with antagonism of GABAa receptors in the brain (Mohamed et al., 2004). Induction of the nuclear receptors PXR, and CAR are associated with the effects of FIP on rodent liver gene expression (Roques et al., 2013). The California Department of Pesticide Regulation selected an acute neurotoxicity study in rats as the regulatory POD for FIP (CDPR, 2023). The study showed decreased hindlimb splay at 2.48 mg/kg after a BMD_{10} (BMDS, version 2.6; BMR = 10) was calculated. A 10-fold factor adjustment was added to extrapolate from rat to human (AdjBMD = 0.25 mg/kg/day) (Table 1).

3.1.3. Propyzamide (PRZ)

An acute oral gavage neurotoxicity study in adult rats showed an increase in landing foot splay (female) and decrease in motor activity (males) only on day one of testing post-treatment at the LOEL of 40 mg/kg/day (US EPA, 2015). There is not currently an MOA for acute PRZ neurotoxicity and there were no other studies in the database showing evidence of neurotoxicity regardless of animal strain or treatment duration. However, initiation of peroxisome proliferation is associated with oxidative stress (Corton et al., 2014), which is also associated with neurotoxicity (Sayre et al., 2008). Effects on motor activity and landing foot-splay were reversed by post-treatment day 2. There was not a no effect level in the study and 40 mg/kg was determined by the US EPA to be the acute oral LOEL (US EPA, 2015) (Table 1). A 10-fold adjustment was added to the LOEL to extrapolate from rat to human (AdjLOEL = 4.0 mg/kg/day).

3.1.4. Carbaryl (CARB)

The acute CARB MOA is through inhibition of AChE in plasma, brain and red blood cells by carbamylation of the serine hydroxyl group at the active site on the enzyme in humans and animals (Moser et al., 2010; US EPA, 2017). Acute AChE inhibition resulted in increased acetylcholine concentrations at the neuronal or neuromuscular synapses in the central and/or peripheral nervous systems and ultimately neurotoxicity seen as decreased neuromuscular function (US EPA, 2017). However, this process is rapidly reversible, allowing for AChE reactivation after a peak inhibition (15–45 min post-treatment) and recovery within minutes or hours (US EPA, 2017). A study in male rats showed increased brain AChE inhibition after a single acute dose of CARB on PND 11 to produce a BMD_{10} of 1.46 mg/kg (Moser et al., 2010; US EPA, 2017) (Table 1). This value was selected for the acute CARB POD. The BMD_{10} was adjusted for 10-fold extrapolation from rat to human (AdjBMD = 0.146 mg/kg).

3.2. Summary of high throughput Transcriptomics, high throughput phenotypic profile and ToxCast data

A summary of the *in vitro* HTTr, HTPP and ToxCast assay data is in Table 2 (Supplemental Tables 1-4). HTTr signatures evaluated in three cell types (MCF-7, U-2 OS, HepaRG) had a range of 218 (PRZ) to 1510 (FIP) gene expression signatures identified and 3 % (CARB) to 5 % (PRZ) with hit-calls of greater than 0.9 (of 1.0) (Harrill et al., 2021). HTPP had 1350 endpoints examined for each chemical in one cell type (U-2 OS) but active hit-calls (>0.9) were only 1 % (FIP, CARB), 5 % (ENDO) and PRZ was inactive at the category level (Nyffeler et al., 2023). While over 1000 ToxCast assays were performed for each chemical, only small percentages were active hit-calls (12–32 %), and even fewer were selected for further analysis (5–11 %) because of relevance to known, or presumptive, metabolic pathways/MOA/AOPs. ToxCast assays were further sorted for neuronal, Phase I/II metabolism and hormonal/endocrine targets to investigate where the most sensitive targets may occur in each category.

3.3. NAMs predictions from Tiers 1–2

Tables 3 to 6 show chemical characterizations using the NAMs for HTTr, HTPP and ToxCast assays, ToxCast Z-Scores, IVIVE predictions (AED_{Human}: mg/kg), and fold differences between predicted AED_{Human} and *in vivo* AdjLOEL/BMDs. Although the cell lines used in the HTTr and HTPP were not neuronal cells, gene expression signatures associated with potential neurotoxicity from ENDO (MCF-7: olfactory nervous system), PRZ (MCF-7: Neurological: Distal sensory impairment), and CARB (HepaRG: Cholinergic) exposures were detected with HTTr assays (Tables 3, 5 and 6). This indicates that neurotoxicity-related transcriptomic gene expression signatures in MCF-7 and U-2 OS were detected even though the treated cells were not specifically neurons. Such activities can be promiscuous and not explicitly associated with a molecular initiating event or they can reveal a gene expression signature associated with neurotoxic effects that warrants further investigation even if it occurs in a non-neuronal cell type (Harrill et al., 2021).

HTPP active hit-calls in U-2 OS cells identified DNA as the most potent target with ENDO and CARB, but mitochondria with FIP. These endpoints in non-neuronal cells may or may not broadly indicate the most sensitive targets regardless of cell type (Tables 3-4 and 6). HTPP was not active with PRZ, and in this case, the method should be interpreted with caution because PRZ was active with HTTr and ToxCast (Table 4).

Z-Scores were calculated only for ToxCast assays because global cytotoxicity MAD and individual chemical cytotoxicity median values in the cytotoxicity burst region were available on the CompTox Chemicals Dashboard and in Judson et al. (2016). Although somewhat similar burst activity, described as “nonspecific bioactivity or cellular stress” (Harrill et al., 2021), occurred in HTTr assays the median cytotoxicity limit reported for HTTr on the CompTox Chemicals Dashboard pertained to values associated with ToxCast assays and not to HTTr (Personal communication J. Harrill, 2023). However, non-specific molecular target-driven transcriptional responses or changes were reported to generally occur at concentrations greater than 10 μM in HTTr assays (Harrill et al., 2021). Assays with Z-Scores were not calculated for the HTPP assay results because, again there was no global cytotoxicity MAD, or median values reported on the CompTox Chemicals Dashboard for the four chemicals examined.

Only assays with Z-Scores of three or greater, indicating chemical-target specificity, were selected for further analysis by 3COMP, PBTK and Fetal PBTK models. Data for either the 3COMP or the PBTK models, performed with adult TK parameters were reported in Tables 3-6, depending on which model produced the lowest FDs. When assays were similar, or identical, but assessed through different gene expression signature sources (HTTr), HTPP categories, or were performed at different timepoints (ToxCast: e.g., CYP assays performed at 6, 12 and

Table 2
Summary of HTTr, HTPP and ToxCast Assay Results.

Parameter	Endosulfan	Fipronil	Propyzamide	Carbaryl
High Throughput Transcriptomics (HTTr): Tier 1				
Total number of active signatures[a]	1307	1510	218	318
High Throughput Phenotypic Profile (HTPP) [b]: Tier 1				
Total Number of Feature Level Endpoints[c]	1300	1300	1300	1300
Total Number of Active Feature-Level Endpoints[c]	497 (38.2 %)	600 (46.1 %)	101 (7.7 %)	337 (25.9 %)
Total Number of Category-Level Endpoints[d]	49	49	49[c]	49
Total Number of Active Category-Level Endpoints[d]	39 (79.5 %)	43 (87.8 %)	0[e]	27 (55.1 %)
BMD of the Most Sensitive Category[e]	0.45 μM	4.96 μM	– [e]	15 μM
Total Number of Global Endpoints[f]	1	1	1	1
Total Number of Active Global Endpoints[f]	1	1	0 [e]	1
BMD of the Global Endpoint	14.74 μM	13.72 μM	–	47.12 μM
Phenotype Altering Concentration (PAC)	0.45 μM	4.96 μM	–	15 μM
ToxCast Assays: Tier 2				
Total Number of Tests Performed	1208	1100	1103	1173
Total Reported Active Hit-Calls (% of Total Tested)	390 (32 %)	334 (30 %)	127 (12 %)	148 (13 %)
Selected Active Hit-calls (% of Total Active) [g]	25 (6 %)	22 (6.5 %)	7 (5 %)	16 (11 %)
Selected Active Hit-Calls Based on Neuronal Targets	13	10	0	2
Selected Active Hit-Calls: Phase I/II Metabolism	5	8	7	12
Selected Active Hit-Calls Based on Hormonal/Endocrine Targets	6	4	0	1
Cytotoxicity Lower Limit (μM)	7.466 μM	7.108 μM	6.701 μM	7.108 μM
Cytotoxicity Median (μM)	42.013 μM	40 μM	37.706 μM	40 μM

a- Active signature hit-calls were ≥ 0.9 of 1.0. There were different transcriptomic signature BMD values for the same target depending upon human cell line tested (e.g., U-2 OS: human osteosarcoma; MCF-7: human mammary adenocarcinoma; HepaRG: biopotential hepatoma-derived cell line).
b- The HTPP was performed in human osteosarcoma cell line: U-2 OS.
c- Each chemical had 1300 feature level endpoints evaluated (e.g., intensity, texture, localization of fluorescent signal, shape, and position of the cells). Active hit-calls were ≥ 0.9.
d- Categories consist of a collection of features or channels (i.e., channel_module_compartmet) and active hit-calls were ≥ 0.9.
e-Categories with the lowest (most sensitive) BMDs were selected for further analysis. PRZ is inactive in the HTPP assay according to the criteria that the global endpoint or at least one category-level endpoint be active (i.e. hit-call ≥ 0.9) to define a Phenotype Altering Concentration (PAC). The total number of endpoints with hitcall ≥ 0.9 are most accurately 101 (7.5 %) and include individual features. However, only category level endpoints were selected for further analysis. The Global BMD for PRZ of 285 μM was above the highest dose tested of 100 μM as shown on the ToxCast Chemicals Dashboard: Propyzamide - Chemical Details (epa.gov)) and the Global Hit-call was 0.0036, which is below the acceptable hit-call cutoff of 0.9 indicating that PRZ was inactive in the HTPP assay.
f-The Global HTPP BMD was made up of all features examined (~1300) and active hit-calls were ≥ 0.9.
g-Active hit-calls were below the cytotoxicity lower limit, with ≤ 2 flags, and were associated with the MOA or metabolic pathway. The assay with the lowest AC_{50} was selected in the case of duplicate assays performed at different time points. Assays performed in humans were selected over the same assay performed in other species, when possible.

Table 3
Endosulfan: HTTr Signatures, HTPP, and ToxCast Modeled Chemical Characterization.

High Throughput Transcriptomic (HTTr) with 3COMP Model: Tier 1					
CELL TYPE	**TARGET/Target Class**	**BMD μM**	**AED_{Human} mg/kg**	**Fold Difference [a,b]**	**Number of Genes in a Transcriptomic Signature Detected in Target Class**
HepaRG	RAR Nuclear Receptor	0.49	0.07	**-2.76**	100
MCF-7	Olfactory Nervous System	2.71	0.36	**+2.0**	69
U-2 OS	EGFR (Epidermal growth factor Receptor) Immune	3.50	0.47	**+2.58**	105
High Throughput Phenotypic Profile (HTPP)[c] with 3COMP Model: Tier 1					
CELL TYPE	**Channel_Module_Compartment**	**BMD μM**	**AED_{Human} mg/kg**	**Fold Difference [a,b]**	**Number of Features[d]**
U-2 OS	DNA_Texture_Nuclei	0.45	0.06	**-3.0**	14
	DNA_Profile_Nuclei	0.62	0.08	**-2.18**	24
TOXCAST[e] with 3COMP Model: Tier 2					
TARGET	**ASSAY NAME**	**AC_{50} μM**	**AED_{Human} mg/kg**	**Fold Difference [a,b]**	**Z-Score[f]**
Nuclear Receptors[g]	ATG_mPXR_XSP1_up	1.05	0.14	**-1.29**	5.53
	ATG_PXRE_CIS_up	1.12	0.15	**-1.21**	5.43
CYP450	CLD_CYP2B6_48hr	1.04	0.14	**-1.30**	5.54
	CLD_CYP3A4_48hr	4.59	0.61	**+3.38**	3.32
	NVS_ADME_hCYP2C19	1.92	0.26	**+1.42**	4.62
Neuro-activity Bursting	CCTE_Shafer_MEA_acute_burst_duration_mean_up	0.316	0.04	**-4.28**	7.32
	CCTE_Shafer_MEA_acute_per_burst_spike_number_mean_up	0.065	0.01	**-21**	9.70
	CCTE_Shafer_MEA_acute_burst_percentage_mean_up	1.93	0.26	**+1.42**	4.61
	CCTE_Shafer_MEA_acute_burst_percentage_std_dn	0.204	0.03	**-6.64**	7.98
Neuro-activity Neural Connectivity	CCTE_Shafer_MEA_acute_per_network_burst_spike_number_std_dn	0.351	0.05	**-3.86**	7.17
	CCTE_Shafer_MEA_acute_network_burst_percentage_up	0.047	0.01	**-29**	10
	CCTE_Shafer_MEA_acute_cross_correlation_HWHM_dn	0.060	0.01	**-22**	9.80
	CCTE_Shafer_MEA_acute_per_network_burst_spike_number_mean_up	0.118	0.02	**-11**	8.80
	CCTE_Shafer_MEA_acute_cross_correlation_area_up	0.669	0.09	**-2.02**	6.20
	CCTE_Shafer_MEA_acute_per_network_burst_electrodes_number_mean_up	1.42	0.19	**1.04**	5.07
DNT Neural Connectivity	CCTE_Shafer_MEA_dev_per_network_spike_spike_percent_dn	4.76	0.63	**+3.51**	3.26
	CCTE_Shafer_MEA_dev_network_spike_number_dn	5.14	0.68	**+3.79**	3.15
Neurodevel	IUF_NPC5_oligodendrocyte_differentiation_120hr_dn	2.91	0.39	**+2.14**	4.00
Nuclear Receptor[h]	TOX21_TSHR_HTRF_Agonist_ratio	4.91	0.65	**+3.62**	3.22
	ATG_ERE_CIS_up	1.35	0.18	**1.00**	5.15
	TOX21_ERa_LUC_VM7_Agonist	4.91	0.65	**+3.63**	3.21
	ATG_hERa_XSP1_up	1.15	0.15	**+1.18**	5.39
	ATG_hERa_XSP2_up	1.43	0.19	**1.06**	5.06
	ATG_ERa_TRANS_up	1.73	0.23	**+1.28**	4.78

a-Fold difference (FD) between *in vivo* AdjPOD (0.18 mg/kg) and 3COMP AED_{Human} mg/kg. The 3COMP model produced AED_{Human} mg/kg PODs closest to *in vivo* AdjPOD for HTTr, HTPP and ToxCast.
b-Analysis by 3COMP modeling using BMDs from HTTr or HTPP assays or AC_{50}s from ToxCast assays.
c-Global BMD: 14.74 μM
d-Number of Features measured in a designated category (Nyffeler 2021)
e-TOXCAST cytotoxicity lower limit/cytotoxicity median: 7.466/42.013 μM
f- Z-Score (chem, assay) = ([-logAC_{50} (chem, assay)] – median [-logAC_{50} (chem, cytotox)]) ÷ Global Cytotox MAD (complete description in Judson et al. (2016)). No Z-Score calculations for HTTr and HTPP due to lack of cytotoxicity median values specific to the HepaRG, MCF-7 and U2OS cell types available on CompTox Chemicals Dashboard.
g-Nuclear receptors related to general xenobiotic metabolism primarily in liver.
h-Nuclear receptors related to endocrine hormone metabolism.
Abbreviations: AC_{50}: concentration at 50% activity; AED_{Human}: administered equivalent dose in humans; BMD: benchmark dose; 3COMP: 3 compartment IVIVE model; CYP: cytochrome P450; DNT: neurodevelopment; ER: estrogen receptor; ERE: estrogen receptor element: FD: fold difference between *in vivo* AdjPOD and predicted AED_{Human} POD; HepaRG: human liver cell line with limited metabolic capacity; HWHM: half width at half maximum for normal distribution; *in vivo* AdjPOD: Adjusted POD = LOEL (0.18 mg/kg) ÷ 10-fold interspecies extrapolation factor (animal to human); IVIVE: *in vitro* to *in vivo* extrapolation; MCF-7: human breast adenocarcinoma cell line; Neurodevel: neurodevelopment; PBTK: physiologically based toxicokinetic; POD: point of departure; PXR/PXRE: pregnane-x-receptor/element; RAR: retinoic acid receptor; TSHR: thyroid stimulating hormone receptor; U-2 OS: human osteosarcoma epithelial cell line.
Shaded: Green: AED_{Human} < *in vivo* AdjPOD ("-"); Yellow: AED_{Human} ≃ *in vivo* AdjPOD; Red: AED_{Human} > *in vivo* AdjPOD ("+")
Red numbers are FD that exceed the optimal 10-fold difference range (Dourson et al., 1996).

a-Fold difference (FD) between *in vivo* AdjPOD (0.18 mg/kg) and 3COMP AED_{Human} mg/kg. The 3COMP model produced AED_{Human} mg/kg PODs closest to *in vivo* AdjPOD for HTTr, HTPP and ToxCast.
b-Analysis by 3COMP modeling using BMDs from HTTr or HTPP assays or AC_{50}s from ToxCast assays.
c-Global BMD: 14.74 μM.
d-Number of Features measured in a designated category (Nyffeler 2021).
e-TOXCAST cytotoxicity lower limit/cytotoxicity median: 7.466/42.013 μM.
f- Z-Score (chem, assay) = ([-logAC_{50} (chem, assay)] – median [-logAC_{50} (chem, cytotox)]) ÷ Global Cytotox MAD (complete description in Judson et al. (2016)). No Z-Score calculations for HTTr and HTPP due to lack of cytotoxicity median values specific to the HepaRG, MCF-7 and U2OS cell types available on CompTox Chemicals Dashboard.
g-Nuclear receptors related to general xenobiotic metabolism primarily in liver.
h-Nuclear receptors related to endocrine hormone metabolism.
Abbreviations: AC_{50}: concentration at 50 % activity; AED_{Human}: administered equivalent dose in humans; BMD: benchmark dose; 3COMP: 3 compartment IVIVE model; CYP: cytochrome P450; DNT: neurodevelopment; ER: estrogen receptor; ERE: estrogen receptor element: FD: fold difference between *in vivo* AdjPOD and predicted AED_{Human} POD; HepaRG: human liver cell line with limited metabolic capacity; HWHM: half width at half maximum for normal distribution; *in vivo* AdjPOD: Adjusted POD = LOEL (0.18 mg/kg) ÷ 10-fold interspecies extrapolation factor (animal to human); IVIVE: *in vitro* to *in vivo* extrapolation; MCF-7: human breast adenocarcinoma cell line; Neurodevel: neurodevelopment; PBTK: physiologically based toxicokinetic; POD: point of departure; PXR/PXRE: pregnane-x-receptor/element; RAR: retinoic acid receptor; TSHR: thyroid stimulating hormone receptor; U-2 OS: human osteosarcoma epithelial cell line.

Shaded: Green: AED_{Human} < *in vivo* AdjPOD ("-"); Yellow: AED_{Human} ≃ *in vivo* AdjPOD; Red: AED_{Human} > *in vivo* AdjPOD ("+").
Red numbers are FD that exceed the optimal 10-fold difference range (Dourson et al., 1996).

Table 4
Fipronil: HTTr Signatures, HTPP, and ToxCast Modeled Chemical Characterization.

High Throughput Transcriptomic (HTTr) with 3COMP Model: Tier 1					
CELL TYPE	**TARGET/Target Class**	**BMD µM**	**AED_{Human} mg/kg**	**Fold Difference [a,b]**	**Number of Genes in a Transcriptomic Signature Detected in Target Class**
MCF-7	mTOR (mammalian target of rapamycin)	1.36	**0.18**	**-1.37**	100
U-2 OS	LI_WILMS_TUMOR_VS_FETAL_KIDNEY_1 (cancer)	0.82	**0.11**	**-2.25**	163
High Throughput Phenotypic Profile (HTPP)[c] with 3COMP Model: Tier 1					
CELL TYPE	**Channel_Module_Compartment**	**BMD µM**	**AED_{Human} mg/kg**	**Fold Difference [a,b]**	**Number of Features[d]**
U-2 OS	Mito_Compactness_Cells	4.96	0.67	**+2.68**	40
TOXCAST[e] with 3COMP Model: Tier 2					
TARGET	**ASSAY NAME**	**AC_{50} µM**	**AED_{Human} mg/kg**	**Fold Difference [a,b]**	**Z-Score[f]**
Nuclear Receptor	ATG_PXRE_CIS_up	5.20	0.70	**+2.82**	**3.05**
CYP450	CLD_CYP2B6_24hr	0.78	0.11	**-2.38**	5.91
	CLD_CYP3A4_48hr	1.35	0.18	**-1.37**	5.08
	NVS_ADME_hCYP2C19	0.70	0.09	**-2.65**	6.06
	NVS_ADME_hCYP2C9	1.04	0.14	**-1.79**	5.47
Transferase	CLD_GSTA2_48hr	4.33	0.59	**+2.34**	3.33
Nuclear Receptor	CLD_SULT2A_48hr	0.19	0.03	**-10**	7.99
Kinase	LTEA_HepaRG_ADK_dn (steatosis)	4.82	0.65	**+1.15**	3.17
Neuro-activity Bursting	CCTE_Shafer_MEA_acute_burst_percentage_mean_up	0.21	0.03	**-9.00**	7.85
	CCTE_Shafer_MEA_acute_per_burst_spike_number_mean_up	0.62	0.08	**-2.98**	6.24
Neuro-activity Neural Connectivity	CCTE_Shafer_MEA_acute_cross_correlation_area_up	2.14	0.29	**+1.16**	4.39
	CCTE_Shafer_MEA_acute_per_network_burst_electrodes_number_mean_up	1.04	0.14	**-1.77**	5.47
	CCTE_Shafer_MEA_acute_per_network_burst_spike_number_mean_up	0.39	0.05	**-5.0**	6.93
	CCTE_Shafer_MEA_acute_synchrony_index_up	1.02	0.14	**-1.81**	5.49
DNT	CCTE_Mundy_HCI_Cortical_Synap&Neur_Matur_BPCount_loss	3.39	0.46	**+1.83**	3.70
DNT	IUF_NPC5_oligodendrocyte_differentiation_120hr_dn	4.72	0.64	**+2.55**	3.20
DNA Binding	TOX21_ARE_BLA_agonist_ratio	4.33	0.59	**+2.34**	3.33
	CCTE_GLTED_hDIO3_dn (deiodinase)	1.16	0.16	**-1.60**	5.31

a-Fold difference (FD) between *in vivo* AdjPOD (0.25 mg/kg) and 3COMP AED_{Human} mg/kg. The 3COMP model produced the AED_{Human} mg/kg PODs closest to *in vivo* AdjPOD for HTTr, HTPP and ToxCast.
b-Analysis by 3COMP modeling using BMDs from HTTr or HTPP assays or AC_{50}s from ToxCast assays.
c-Global BMD: 13.72 µM
d- Number of Features measured in the designated category (Nyffeler 2021)
e- TOXCAST cytotoxicity lower limit/cytotoxicity median: 7.108/42.01
f- Z-Score (chem, assay) = ([-logAC50 (chem, assay)] – median [-logAC_{50} (chem, cytotox)]) ÷ Global Cytotox MAD (complete description in Judson et al. (2016)). No Z-Score calculations for HTTr and HTPP due to lack of cytotoxicity median values reported on CompTox Chemicals Dashboard.
Abbreviations: AC_{50}: concentration at 50% activity; Adj: Adjusted; AED_{Human}: administered equivalent dose in humans; ADK: adenosine kinase (marker of steatosis); ARE: androgen receptor element; BMD: benchmark dose; 3COMP: 3 compartment IVIVE model; CYP: cytochrome P450; hDIO3: human deiodinase; DNT: developmental neurotoxicity; FD: fold difference between *in vivo* AdjPOD and predicted AED_{Human} POD; GSTA: glutathione-s-transferase; HepaRG: biopotential hepatoma-derived cell line; *in vivo* AdjPOD: Adjusted POD = LOEL (0.25 mg/kg) ÷ 10-fold interspecies extrapolation factor (animal to human); IVIVE: *in vitro* to *in vivo* extrapolation; MCF-7: human breast cancer cell line; PXRE: pregnane x receptor element; SULTA: sulfotransferase; U-2 OS: human osteosarcoma epithelial cell line
Shaded: Green: AED_{Human} < *in vivo* AdjPOD ("-"); Yellow: AED_{Human} ≃ *in vivo* AdjPOD; Red: AED_{Human} > *in vivo* AdjPOD ("+")

a-Fold difference (FD) between *in vivo* AdjPOD (0.25 mg/kg) and 3COMP AED_{Human} mg/kg. The 3COMP model produced the AED_{Human} mg/kg PODs closest to *in vivo* AdjPOD for HTTr, HTPP and ToxCast.
b-Analysis by 3COMP modeling using BMDs from HTTr or HTPP assays or AC_{50}s from ToxCast assays.
c-Global BMD: 13.72 µM.
d- Number of Features measured in the designated category (Nyffeler 2021).
e- TOXCAST cytotoxicity lower limit/cytotoxicity median: 7.108/42.01.
f- Z-Score (chem, assay) = ([-logAC50 (chem, assay)] – median [-logAC_{50} (chem, cytotox)]) ÷ Global Cytotox MAD (complete description in Judson et al. (2016)). No Z-Score calculations for HTTr and HTPP due to lack of cytotoxicity median values reported on CompTox Chemicals Dashboard.
Abbreviations: AC_{50}: concentration at 50 % activity; Adj: Adjusted; AED_{Human}: administered equivalent dose in humans; ADK: adenosine kinase (marker of steatosis); ARE: androgen receptor element; BMD: benchmark dose; 3COMP: 3 compartment IVIVE model; CYP: cytochrome P450; hDIO3: human deiodinase; DNT: developmental neurotoxicity; FD: fold difference between *in vivo* AdjPOD and predicted AED_{Human} POD; GSTA: glutathione-s-transferase; HepaRG: biopotential hepatoma-derived cell line; *in vivo* AdjPOD: Adjusted POD = LOEL (0.25 mg/kg) ÷ 10-fold interspecies extrapolation factor (animal to human); IVIVE: *in vitro* to *in vivo* extrapolation; MCF-7: human breast cancer cell line; PXRE: pregnane x receptor element; SULTA: sulfotransferase; U-2 OS: human osteosarcoma epithelial cell line.
Shaded: Green: AED_{Human} < *in vivo* AdjPOD ("-"); Yellow: AED_{Human} ≃ *in vivo* AdjPOD; Red: AED_{Human} > *in vivo* AdjPOD ("+").

24 h), only results with the lowest BMDs or AC_{50}s were selected as model inputs. ICE Models that were selected as the most predictive produced AED_{Human} values with FD that were closest to the *in vivo* AdjLOEL/BMDs (Supplemental Table 5).

3.3.1. Endosulfan

The 3COMP model with ENDO had the lowest FD between the AED_{Human} predictions compared to the *in vivo* AdjLOEL using the HTTr, HTPP and ToxCast assay model inputs (Table 3). The PBTK modeled AED_{Human} predicted FD were, generally about 170 % greater than those generated by the 3COMP model across the three assay methods (Supplemental Tables 1 and 4).

HTTr (Tier 1): ENDO was tested with three cell types (MCF-7, U-2OS, HepaRG). The lowest HTTr BPAC was for the RAR (retinoid acid receptor) nuclear receptor gene (BMD: 0.49 µM) in HepaRG (Table 3). RARs are involved with vertebrate development (i.e., embryonic

Table 5
Propyzamide: HTTr Signatures and ToxCast Modeled Chemical Characterization.

High Throughput Transcriptomic (HTTr) with the PBTK Model: Tier 1					
CELL TYPE	**TARGET/Target Class**	**BMD µM**	**AED_{Human} mg/kg**	**Fold Difference [a,b]**	**Number of Genes Detected in Target Class**
MCF-7	CYP P450	2.34	0.29	**-6.57**	100
MCF-7	Developmental Processes	0.49	0.06	**-31**	190
MCF-7	Neurological: Distal sensory impairment	1.85	0.23	**-8.32**	79
MCF-7	Stress: DNA100	0.38	0.05	**-31**	100
High Throughput Phenotypic Profile (HTPP)[c]: Tier 1					
CELL TYPE	**Channel_Module_Compartment**	**BMD µM**	**AED_{Human} mg/kg**	**Fold Difference [a,b]**	**Number of Features[d]**
Not Applicable	No hit-calls <0.9	--	--	--	--
TOXCAST[e] with PBTK Model: Tier 2					
TARGET	**ASSAY NAME**	**AC_{50} µM**	**AED_{Human} mg/kg**	**Fold Difference [a,b]**	**Z-Score[f]**
CYPP450	NVS_ADME_hCYP1A1	2.31	0.28	**-6.67**	4.18
	CLD_CYP1A2_48hr	0.43	0.05	**-36**	6.70
	NVS_ADME_rCYP2A1	1.96	0.24	**-7.86**	4.43
	CLD_CYP2B6_48hr	3.71	0.46	**-4.15**	3.47
	NVS_ADME_hCYP2J2	1.65	0.20	**-3.92**	4.69
	LTEA_HepaRG_CYP3A7_up	4.60	0.57	**-3.34**	3.15
Transferase	CLD_UGT1A1_24hr	1.69	0.21	**-9.11**	4.65

a- Fold difference (FD) between *in vivo* AdjPOD (4.0 mg/kg) and PBTK AED_{Human} mg/kg. The PBTK model produced the AED_{Human} mg/kg PODs closest to *in vivo* AdjPOD with HTTr and ToxCast.
b-Analysis by PBTK modeling using BMDs from HTTr or AC_{50}s from ToxCast assays.
c- The highest hit-call for HTPP was AGP_Axial_Cells at 0.65. The hit-call below the cutoff rendered the HTTP method inactive (data not reliable) for PRZ.
d- Number of Features measured in the designated category (Nyffeler 2021)
e- TOXCAST cytotoxicity lower limit/cytotoxicity median: 6.7/37.7 µM
f- Z-Score (chem, assay) = ([-logAC_{50} (chem, assay)] – median [-logAC_{50} (chem, cytotox)]) ÷ Global Cytotox MAD (complete description in Judson et al. (2016)). No Z-Score calculations for HTTr and HTPP due to lack of cytotoxicity median values reported on CompTox Chemicals Dashboard
Abbreviations: AC_{50}: concentration at 50% activity; Adj: Adjusted; Adj: Adjusted; ADR: alpha-1A adrenergic receptor; AED_{Human}: administered equivalent dose in humans; BMD: benchmark dose; CYP: cytochrome P450; FD: fold difference between *in vivo* AdjPOD and predicted AED_{Human} POD; *in vivo* AdjPOD: Adjusted POD = LOEL (4.0 mg/kg) ÷ 10-fold interspecies extrapolation factor (animal to human); HepaRG: biopotential hepatoma-derived cell line; IVIVE: *in vitro* to *in vivo* extrapolation; MCF-7: human breast cancer cell line; PBPK: Physiologically Based Toxicokinetic; UGT1A1: UDP glucuronosyltransferase: U-2 OS: human osteosarcoma epithelial cell line
Shaded: Green: AED_{Human} < *in vivo* AdjPOD ("-"); Red: AED_{Human} > *in vivo* AdjPOD ("+")
Red numbers are FD that exceed the optimal 10-fold difference range (Dourson et al., 1996).

a- Fold difference (FD) between *in vivo* AdjPOD (4.0 mg/kg) and PBTK AED_{Human} mg/kg. The PBTK model produced the AED_{Human} mg/kg PODs closest to *in vivo* AdjPOD with HTTr and ToxCast.
b-Analysis by PBTK modeling using BMDs from HTTr or AC_{50}s from ToxCast assays.
c- The highest hit-call for HTPP was AGP_Axial_Cells at 0.65. The hit-call below the cutoff rendered the HTTP method inactive (data not reliable) for PRZ.
d- Number of Features measured in the designated category (Nyffeler 2021).
e- TOXCAST cytotoxicity lower limit/cytotoxicity median: 6.7/37.7 µM.
f- Z-Score (chem, assay) = ([-logAC_{50} (chem, assay)] – median [-logAC_{50} (chem, cytotox)]) ÷ Global Cytotox MAD (complete description in Judson et al. (2016)). No Z-Score calculations for HTTr and HTPP due to lack of cytotoxicity median values reported on CompTox Chemicals Dashboard.
Abbreviations: AC_{50}: concentration at 50 % activity; Adj: Adjusted; Adj: Adjusted; ADR: alpha-1A adrenergic receptor; AED_{Human}: administered equivalent dose in humans; BMD: benchmark dose; CYP: cytochrome P450; FD: fold difference between *in vivo* AdjPOD and predicted AED_{Human} POD; *in vivo* AdjPOD: Adjusted POD = LOEL (4.0 mg/kg) ÷ 10-fold interspecies extrapolation factor (animal to human); HepaRG: biopotential hepatoma-derived cell line; IVIVE: *in vitro* to *in vivo* extrapolation; MCF-7: human breast cancer cell line; PBPK: Physiologically Based Toxicokinetic; UGT1A1: UDP glucuronosyltransferase: U-2 OS: human osteosarcoma epithelial cell line.
Shaded: Green: AED_{Human} < *in vivo* AdjPOD ("-"); Red: AED_{Human} > *in vivo* AdjPOD ("+").
Red numbers are FD that exceed the optimal 10-fold difference range (Dourson et al., 1996).

morphogenesis, organogenesis, differentiation, apoptosis, and others) and genetic disruptions are associated with human carcinomas and dermatological diseases (Germain et al., 2006). Although RAR genes are not specifically identified with a GABAa receptor AOP (Abalis et al., 1986; Casida, 1993; Ffrench-Constant et al., 2000; Lawrence & Casida, 1984), these genes are associated with critical biological processes.

MCF-7 and U-2 OS cell lines had higher BMD values at 2.71 and 3.50 µM, respectively as their lowest BPAC; affecting HTTr gene expression signatures for olfactory nervous system and the epidermal growth factor receptor (EGFR: immune-related) pathway has 105 genes in a gene expression signature (NUM_GENES: Supplemental Table 1) (Harrill et al., 2021). The MCF-7 gene expression signature with the lowest BMD was for the olfactory nervous system (Table 3; Supplemental Tables 1 and 5). ENDO affects neurotransmission within the olfactory bulb in rats (Lakshmana & Raju, 1994) where there are mainly GABAbeta and estrogen-beta (ESR2) receptors (Mazo et al., 2016; Schantz & Widholm, 2001). MCF-7 cells are enriched in ESR1 and ESR2 receptors and ENDO is weakly estrogenic in these cells (Soto et al., 1994).

U-2 OS lowest gene expression activity (3.50 µM) corresponded to immune-associated EGFR (Table 3, Supplemental Tables 1 and 5) after 105 genes were assessed in a transcriptomic signature (Harrill et al., 2021). Mutations in the immune-associated EGFR gene can affect inflammation in skin diseases such as eczema and psoriasis (as does RAR), in addition to affecting numerous forms of epithelial cancers (e.g., breast, lung, colon) (Sasaki et al., 2013). Overall, ENDO identified gene expression signatures in two cell lines that could potentially lead to dermatological diseases (HepaRG: RAR and U-2 OS: EGFR).

The FD were all less than five between the *in vivo* (Table 1; AdjLOEL: 0.18 mg/kg) and AED_{Human} predicted by the 3COMP model for the three cell lines (Table 3). The FD between the RAR nuclear receptor AED_{Human} and the *in vivo* AdjLOEL was less than one at −2.76, whereas the other two were greater than one (+2.0: olfactory nervous system and + 2.58 EGFR immune); each indicating high concordance.

HTPP (Tier 1): DNA was the main target for ENDO in the HTPP assay (Table 3). It was most active or had the lowest PAC with U-2 OS cells in the DNA "channel", with altered texture "module" in the nuclei "compartment" (DNA_Texture_Nuclei; BMD: 0.45 µM; 14 features examined) (Table 3). However, the DNA "channel", and profile

Table 6
Carbaryl: HTTr Signatures, HTPP, and ToxCast Modeled Chemical Characterization.

High Throughput Transcriptomic (HTTr) with the 3COMP Model: Tier 1					
CELL TYPE	**TARGET/Target Class**	**BMD μM**	**AED_{Human} mg/kg**	**Fold Difference [a,b]**	**Number of Genes Detected in Target Class**
MCF-7	ETS1: transcription factor	0.60	2.06	**+14**	137
HepaRG	Cholinergic	4.64	0.27	**+1.85**	100
U-2 OS	SREBF (sterol regulatory element-binding TF)	0.95	0.42	**+2.88**	21
High Throughput Phenotypic Profile (HTPP)[c] with 3COMP Model: Tier 1					
CELL TYPE	**Channel_Module_Compartment**	**BMD μM**	**AED_{Human} mg/kg**	**Fold Difference [a,b]**	**Number of Features[d]**
U-2 OS	DNA_Texture_Nuclei	15	6.63	**+45**	14
TOXCAST[e] with 3COMP Model: Tier 2					
TARGET	**ASSAY NAME**	**AC_{50} μM**	**AED_{Human} mg/kg**	**Fold Difference [a,b]**	**Z-Score[f]**
Nuclear Receptor	TOX21_AhR_LUC_Agonist	3.88	1.72	**+12**	3.49
CYP450	CLD_CYP1A1_48hr	4.31	1.91	**+13**	3.34
	CLD_CYP1A2_24hr	2.83	1.25	**+8.56**	3.97
	CLD_CYP2B6_48hr	4.42	1.95	**+13**	3.30
	NVS_ADME_hCYP19A1	3.43	1.52	**+10**	3.68
Metabolite/DNT	STM_H9_OrnCyssISnorm_ratio_dn	2.69	1.19	**+8.14**	4.05
	STM_H9_CystinelSnorm_perc_up	2.87	1.27	**+8.70**	3.94
DNT General Neuronal Activity	CCTE_Shafer_MEA_dev_firing_rate_mean_dn	1.90	0.84	**+5.77**	4.56
DNT Neural Connectivity	CCTE_Shafer_MEA_dev_network_spike_number_dn	1.40	0.62	**+4.23**	5.02
Esterase	NVS_ENZ_rAChE	7.37	3.26	**+22**	2.53

a- Fold difference (FD) between *in vivo* AdjPOD (0.146 mg/kg) and 3COMP AED_{Human} mg/kg PODs. The 3COMP model produced AED_{Human} mg/kg PODs closest to *in vivo* AdjPOD for HTTr, HTPP and ToxCast.
b-Analysis by 3COMP or PBTK modeling using BMDs from HTTr or HTPP assays or AC_{50}s from ToxCast assays.
c-Global BMD: 47 μM
d-Number of Features measured in the designated category (Nyffeler 2021)
e-TOXCAST cytotoxicity lower limit/cytotoxicity median: 7.466/53.722 μM
f- Z-Score (chem, assay) = ([-logAC_{50} (chem, assay)] – median [-logAC50 (chem, cytotox)]) ÷ Global Cytotox MAD (complete description in Judson et al. (2016)). No Z-Score calculations for HTTr and HTPP due to lack of cytotoxicity median values reported on CompTox Chemicals Dashboard
Abbreviations: AC_{50}: concentration at 50% activity; Adj: Adjusted; AED_{Human}: administered equivalent dose in humans; BMD: benchmark dose; 3COMP: 3 compartment IVIVE model; CYP: cytochrome P450; DNT: developmental neurotoxicity; FD: fold difference between *in vivo* Adjusted POD and predicted AED_{Human} POD; HepaRG: human liver cell line with limited metabolic capacity; *in vivo* AdjPOD: Adjusted POD = LOEL (0.146 mg/kg) ÷ 10-fold interspecies extrapolation factor (animal to human); IVIVE: *in vitro* to *in vivo* extrapolation; MCF7: human breast cancer cell line; OrnCyssISnorm: developmental biomarker for ratio or percent change in metabolites for CARB; POD: point of departure; PXR/PXRE: pregnane X receptor/element; U-2 OS: human osteosarcoma epithelial cell line
Shaded: Red: AED_{Human} > *in vivo* AdjPOD ("+")
Red numbers are FD that exceed the optimal 10-fold difference range (Dourson et al., 1996).

a- Fold difference (FD) between *in vivo* AdjPOD (0.146 mg/kg) and 3COMP AED_{Human} mg/kg PODs. The 3COMP model produced AED_{Human} mg/kg PODs closest to *in vivo* AdjPOD for HTTr, HTPP and ToxCast.
b-Analysis by 3COMP or PBTK modeling using BMDs from HTTr or HTPP assays or AC_{50}s from ToxCast assays.
c-Global BMD: 47 μM.
d-Number of Features measured in the designated category (Nyffeler 2021).
e-TOXCAST cytotoxicity lower limit/cytotoxicity median: 7.466/53.722 μM.
f- Z-Score (chem, assay) = ([-logAC_{50} (chem, assay)] – median [-logAC50 (chem, cytotox)]) ÷ Global Cytotox MAD (complete description in Judson et al. (2016)). No Z-Score calculations for HTTr and HTPP due to lack of cytotoxicity median values reported on CompTox Chemicals Dashboard.
Abbreviations: AC_{50}: concentration at 50 % activity; Adj: Adjusted; AED_{Human}: administered equivalent dose in humans; BMD: benchmark dose; 3COMP: 3 compartment IVIVE model; CYP: cytochrome P450; DNT: developmental neurotoxicity; FD: fold difference between *in vivo* Adjusted POD and predicted AED_{Human} POD; HepaRG: human liver cell line with limited metabolic capacity; *in vivo* AdjPOD: Adjusted POD = LOEL (0.146 mg/kg) ÷ 10-fold interspecies extrapolation factor (animal to human); IVIVE: *in vitro* to *in vivo* extrapolation; MCF7: human breast cancer cell line; OrnCyssISnorm: developmental biomarker for ratio or percent change in metabolites for CARB; POD: point of departure; PXR/PXRE: pregnane X receptor/element; U-2 OS: human osteosarcoma epithelial cell line.
Shaded: Red: AED_{Human} > *in vivo* AdjPOD ("+").
Red numbers are FD that exceed the optimal 10-fold difference range (Dourson et al., 1996).

"module" in the nuclei "compartment" (DNA_Profile_Nuclei; BMD: 0.62 μM; 24 features examined) was almost equally sensitive (Table 3; Supplemental Tables 1 and 5). The "global" endpoint was 14.74 μM, 97 % (30-fold) higher than the lowest BMD of 0.45 μM. Both HTPP assay results had AED_{Human} PODs < 5 FD from the *in vivo* AdjPOD indicating high concordance with the 3COMP model. The HTPP assay detected DNA as a critical endpoint that may occur in neurons as well as U-2 OS cells. This is a hypothesis that needs to be tested.

ToxCast (Tier 2): ENDO had active hit-calls for targets that were directly relevant to ENDO metabolism (e.g.,[CYP2B6, CYP3A4: human liver primary cells], [PXR and PXRE: HepG2]) (Bebe & Panemangalore, 2003; Casabar et al., 2006; Ihunnah et al., 2011; Pavek & Dvorak, 2008). A cell-free assay for human CYP2C19, a xenobiotic metabolizing enzyme, was also active with ENDO but it is not specifically associated with the MOA (Flockhart, 1995). The selected assay AC_{50}s were below the cytotoxicity lower limit (7.46 μM) (Tables 2-3). The AED_{Human} predictions indicated high concordance, ranging from −1.21 FD below to + 3.38 FD above the *in vivo* AdjPOD (0.18 mg/kg) with the 3COMP model.

There were 10 acute neuroactivity assay endpoints, two developmental neurotoxicity (DNT) performed in rat cortical cells and one neurodevelopmental assay (hNPC brain cells) comprising 13 of 25 (52 %) total selected active hit-calls for ENDO. Neural connectivity (8 of 13 total assays; 62 %) was the most affected target for acute neuroactivity and DNT assays (Shafer, 2021; Shafer et al., 2019). The lowest AC_{50}s occurred with acute neuroactivity bursting (1) and connectivity (3) assays indicating an area of acute sensitivity in rat cortical neurons (Robinette et al., 2011). The lowest acute neuroactivity "bursting" category AC_{50} was 0.065 μM ("up"), with an AED_{Human} that was 21 FD lower than the *in vivo* AdjLOEL (low concordance). The lowest acute neuroactivity AC_{50}s in the "neural connectivity" category were for network burst percentage "up" (0.047 μM), percentage burst spike

number mean "up" (0.118 μM), and a decrease ("dn") in cross correlation area (half width at half maximum [HWHM] of cross-correlogram/well; 0.060 μM). AED_{Human} for these three assays showed FD of 29, 11 and 22, respectively, below the *in vivo* AdjLOEL, exceeding the optimal prediction range (~10 FD) (Dourson et al., 1996). Increased ("up") activities support the increased *in vivo* acute GABA-related ENDO hyperactivity and convulsions seen in rabbits (CDPR, 2008; Silva & Gammon, 2009). Higher AC_{50}s with DNT assays (lesser toxicity) are in the "dn" direction, indicating decreased percent of spikes in network spikes and disruption in coordinated neural network activity. ENDO was active in the "dn" direction in a developmental assay with primary human fetal neural progenitor cells (hNPC5: IUF_NPC5_oligodendrocyte_differentiation_120hr_dn). In this assay human fetal hNPC cell spheres migrate and differentiate into oligodendrocytes. Disruptions in hNPC5 oligodendrocyte differentiation could affect the structure of axonal myelination in the central nervous system (Baumann & Pham-Dinh, 2001). The predicted AED_{Human} values were below or approximately equal to the *in vivo* AdjPOD in all but one of the neuronal assays with a range of −29 FD below (low concordance) to + 1.42 FD (high concordance) above with the 3COMP model. Although the ENDO MOA is blocking of ion channels at the GABA receptor site, it was inactive in a cell-free (Novascreen) bovine GABA receptor A5 assay (NVS_LGIC_b-GABARa5) on the CompTox Chemicals Dashboard (only GABA assay tested; version 2.2.1; Supplemental Tables 1 and 5). The GABA assays, especially the cell-free assays may not have the parameters needed for the chemical-target interaction. In addition it is the GABAa, subunit b3 that is most sensitive to ENDO, not the GABAa5, which was tested and that might explain the lack of activity (Ratra et al., 2001).

Endocrine-related nuclear receptor target families had active hit-calls for thyroid, ER (HepG2 and VM7 ovary cells), and specifically ERa with AC_{50}s below the cytotoxicity limit (Supplemental Tables 1 and 5). It is well-documented that *in vivo* ENDO treatment affects estrogenic pathways (Silva & Gammon, 2009; Silva et al., 2015). Although the TSHR is not known to be part of the ENDO MOA (CDPR, 2008; US EPA, 2002a), an acute high dose of ENDO in pubertal male rats (6.12 mg/kg/day) resulted in down regulation of thyroid stimulating hormone (TSH) along with decreased plasma concentrations (Caride et al., 2010). These effects were associated with pituitary toxicity, since TSH expression is modified by ENDO. With the 3COMP model, endocrine AED_{Human} values had 50 % of assays (2/6) that were equivalent to *in vivo* AdjPOD (~1 FD) and the remaining 4 assays had + 1.18 to + 3.63 FD. For ENDO the 3COMP model was highly concordant with AdjPOD observed *in vivo* (Table 3). Z-Scores for all selected ToxCast assays were greater than three, showing the likelihood of chemical-target specificity.

3.3.2. *Fipronil*

The 3COMP model with FIP had the lowest FD between the AED_{Human} predictions compared to the *in vivo* AdjBMD using the HTTr, HTPP and ToxCast assay model inputs. The PBTK modeled AED_{Human} predicted FD were, generally about 200 % greater than those generated by the 3COMP model across the three assay methods (Supplemental Tables 1 and 5).

HTTr (Tier 1): FIP was tested in the three cell types (MCF-7, U-2 OS, HepaRG). U-2 OS cells had the lowest HTTr BPAC (BMD: 0.82 μM) with the "LI_WILMS_TUMOR_VS_FETAL_KIDNEY_1 (cancer)" signature indicating genes downregulated in Wilm's tumor samples compared to fetal kidney (163 genes in a gene expression signature; Table 4; Supplemental Tables 1 and 5) (Harrill et al., 2021). FIP is not associated with Wilm's tumor in kidney, as it is considered a genetic disease not known to be induced by environmental chemicals (Anvar et al., 2019). The next higher BPAC signature (BMD: 1.36 μM) was in MCF-7 cells with an mTOR (mammalian target of rapamycin) gene expression signature (100 genes: Table 4). "mTOR" regulates cellular processes for cell growth, proliferation, motility, survival, protein synthesis, transcription, and homeostasis (Lipton & Sahin, 2014; Tokunaga et al., 2004). The mTOR gene affects many metabolic pathways, such that perturbation by FIP is likely incidental and not chemical-specific. FIP had a gene expression signature in MCF-7 cells for a "neuron" target in the "nervous system" Target Class, but the BMD was 11 μM which is much higher than the BPAC at 0.82 μM. A BMD of > 10 μM in HTTr assays is likely non-specific and could be within the burst region (Harrill et al., 2021). The lowest gene expression signature BMD in HepaRG cells (Random_340) was 4.89 mg/kg. The context is that in Harrill et al. (2021) 1000 random signatures, or "random sets of genes with the same gene co-occurrence frequency and signature length distribution as the collection of real signatures" to compare to known signatures associated with 41 chemicals tested. "Target", "Target Class" and "Target Level" were all described as "random" and did not provide meaningful information for FIP characterization. With the 3COMP models, both assays showed FD −2.25 to −1.37 below the *in vivo* AED_{Human}, indicating high concordance. Neurotoxic gene expression signatures were not detected in the cells available in this test system.

HTPP (Tier 1): FIP was tested in U-2 OS cells only. The most sensitive effects were associated with mitochondrial morphology for FIP in the HTPP assay (Table 4; Supplemental Tables 1 and 5). It had the lowest PAC with U-2 OS cells in the mitochondria "channel", with altered compactness "module" in U-2 OS cells "compartment" (Mito_-Compactness_Cells; BMD: 4.96 μM; 40 features examined) (Table 4). Compactness describes how tightly packed the brightest features inside an object are using various thresholds (e.g., 30 %) (Harrill et al., 2021; Nyffeler et al., 2023; Nyffeler et al., 2020; Thomas et al., 2019). FIP administered by gavage to male Wistar rats for 28 days results in loss of spermatozoa mitochondrial membrane potential and increased cell death at a LOEL of 2.5 mg/kg/day (Khan et al., 2015). However, it is not specifically known whether a loss of mitochondrial membrane potential (a functional endpoint) results in a change in mitochondrial compactness (a morphological endpoint) that would resemble qualitatively the effects of FIP in the U-2 OS cells. The global BMD of 13.72 μM, exceeding the PAC BMD of 4.96 μM which was used for further analysis. The AED_{Human} for HTPP Mito_Compactness_Cells assay was + 2.68 FD above *in vivo* $AdjBMD_{10}$ (high concordance) with the 3COMP model. Neurotoxic endpoints were not detected in the cells available in this test system.

ToxCast (Tier 2): FIP had active hit-calls for targets that were directly relevant to metabolic pathways with PXRE (HepG2 cells), CYP2B6 and CYP3A4 (primary human hepatocytes), and cell free human CYP2C19 and CYP2C9 assays (Abass et al., 2012; Tang et al., 2004) (Table 4). FIP is metabolized primarily by CYP3A4 with human liver microsomes to form fipronil-sulfone, the major metabolite (Carrão et al., 2019).

FIP Phase II metabolism showed induction of transporters UGT1a1 and SULT1b1 based on mRNA microarrays (Roques et al., 2013). ToxCast Phase II metabolism showed FIP active hit-calls with glutathione-S-transferase (GSTA2: primary human liver) and sulfotransferase-2A (SULT2A: primary human liver; Table 4; Supplemental Tables 1 and 5). GST was depleted in male Wistar rats treated by gavage with 5 mg/kg FIP for 14 days (Mazzo et al., 2018). SULT2, regulated by CAR, when upregulated leads to conjugation and elimination of substrates into bile and feces. These metabolic steps support the *in vivo* findings where increased metabolism and excretion of thyroid hormone occur from FIP treatment in rodents (Roques et al., 2012). FIP was active with adenosine kinase (ADK in HepaRG), a marker of steatosis (Boison et al., 2002). FIP increased fatty liver and associated pathologies in rodents (Ferreira et al., 2012; Roques et al., 2012). The AED_{Human} predictions for Phase I and II metabolism, except for ADK and GSTA2, had FD below the *in vivo* AdjBMD ranging from −10 (concordant) to −1.37 (high concordance). The FD values greater than the *in vivo* AdjBMD were + 1.15 (ADK steatosis) and + 2.34 (GSTA2), but all FD had high concordance (≤5) or were concordant at > 5 ≤ 10) in the 3COMP model.

Almost half of the selected active hit-calls for FIP were for neuronal effects (8/18; 44 %) mainly for increased ("up") acute neuroactivity (6/8; 75 %) associated with neural connectivity (4) and bursting (2). FIP is a

GABA-gated chloride channel inhibitor, with neurotoxicity as the primary MOA (Cole et al., 1993; Hainzl et al., 1998). The reversible, non-competitive blockage of chloride ions through GABAa receptors in the CNS can result in seizures (Mohamed et al., 2004), which supports the increased activity in the acute neuroactivity ToxCast results. The neurodevelopmental assay (CCTE_Mundy_HCI_Cortical_Synap&Neur_Matur_BPCount_loss) measured synaptogenesis and neurite maturation related to number of branch points in neurons from primary rat cortical cells. FIP was active in the "dn" direction in a developmental assay with hNPC5 neural progenitor cells (IUF_NPC5_oligodendrocyte_differentiation_120hr_dn). The human fetal hNPC cell spheres migrate and differentiate into oligodendrocytes and FIP was shown to decrease these processes. Decreases in cortical synaptogenesis, neurite maturation and hNPC5 oligodendrocyte differentiation could affect the neuronal connectivity in the CNS (Baumann & Pham-Dinh, 2001).

AED_{Human} predictions for the six neuroactivity assays had FD less than the *in vivo* AdjBMD in a range of −9.0 to + 1.16. The two neurodevelopmental assays predictions slightly overestimated the *in vivo* AdjBMD (FD: +1.83, +2.55) (Table 4). Overall, the 3COMP model had high concordance based on the low FD. Although the FIP MOA directly involves binding at the GABA receptor site, FIP was not reported to have been tested in GABA assays on the CompTox Chemicals Dashboard (version 2.2.1; Supplemental Tables 1 and 5).

Endocrine ToxCast results had active hit-calls in the androgen receptor element (ARE: HepG2 cells) agonist assay, although this nuclear receptor is not generally a target for FIP. On the other hand, the inhibition of the human iodothyronine deiodinase type 3 (DIO3) enzyme (CCTE_GLTED_hDIO3_dn (deiodinase) in a cell-free assay is relevant to the FIP MOA (Roques et al., 2013). DIO3 (iodothyronine) deactivates thyroid hormone (T4) and turns it into an inactive metabolite reverse T3 (rT3) (Sabatino et al., 2021). The sources of active hormone are depleted by deiodination of the inner ring of T4 and T3 to regulate circulating fetal thyroid hormone concentrations and prevent premature exposure of fetal tissues to adult levels of thyroid hormones (Gutiérrez-Vega et al., 2020). FIP AED_{Human} with the androgen receptor element and the DIO3 assays were + 2.34 and −1.60 (high concordance), respectively with the 3COMP model. All the Z-Scores for ToxCast assays were greater than three indicating the likelihood of a chemical-target specificity (Table 4; Supplemental Tables 1 and 5). However, activity with the nuclear receptor "ARE" in HepG2 liver cell line is not seen with FIP *in vivo* where complete metabolic processes are available.

3.3.3. Propyzamide

The more complex (7 compartment) PBTK model with PRZ had the lowest FD between the AED_{Human} predictions compared to the *in vivo* AdjLOEL with HTTr, and ToxCast assay model inputs. The 3COMP modeled AED_{Human} predicted FD were, generally about 212 % greater than those generated by the PBTK model across the two assay methods (Supplemental Tables 1 and 5). HTPP was inactive with PRZ.

HTTr (Tier 1): PRZ was tested in the three cell types (MCF-7, U-2 OS, HepaRG). MCF-7 cells treated with PRZ showed the lowest HTTr BPACs were signatures for stress ("Bryant Stress Signatures"; BMD = 0.38 μM (100 genes in a transcriptomic signature) (Harrill et al., 2021) and for developmental processes with mesenchymal progression from formation to the mature structure (190 genes in a transcriptomic signature; BMD = 0.49 μM (Table 5; Supplemental Tables 1 and 5). PRZ is associated with stress enzymes through peroxisome proliferation receptor alpha (PPAR-α,) associated with biomarkers for peroxisome proliferation (LeBaron et al., 2014). Peroxisomes contain enzymes related to oxidative stress (catalase, D-amino acid oxidase, uric acid oxidase). PRZ is not currently associated with developmental effects. However, fold difference for an HTTr gene expression signature was −31 (below the *in vivo* AdjLOEL), which could indicate it is a sensitive target. On the other hand, such large FD with a target that was not associated with PRZ toxicity, indicates a likely incidental effect. The signatures for CYP450 (BMD = 2.34 μM) are related to acute *in vivo* Key Events for PRZ toxicity (100 genes in a transcriptomic signature) (Harrill et al., 2021; LeBaron et al., 2014) and neurological activity (79 genes in a transcriptomic signature; "distal sensory impairment"; BMD = 1.85 μM) (Harrill et al., 2021) is directly associated with acute *in vivo* observations (decreased motor activity) (Andrus & Hukkanen, 2011). HepaRG cells had the most potent (lowest) BMD, but the target was "random" and hence, not associated with PRZ characterization. The lowest gene expression signature with U-2 OS cells was for an antimicrobial pesticide (methyl-benzethonium chloride) according to the assay description (Supplemental Tables 1 and 5).

The AED_{Human} FD for the CYP P450 and neurological activity signatures with the PBTK model were −6.57 and −8.37 below the *in vivo* AdjLOEL, respectively, indicating concordance with the *in vivo* AdjPOD.

HTPP (Tier 1): PRZ was tested with U-2 OS cells only. The main target for PRZ was "actin, golgi and plasma membrane" (AGP) in the HTPP assay (Table 5; Supplemental Tables 1 and 5). It was most active and had the lowest PAC with U-2 OS cells in the AGP "channel", with altered axial orientation "module" in U-2 OS cells "compartment" (AGP_Axial_Cells; BMD: 57 μM; 20 features examined) (Table 5). However, since the highest hit-call was 0.65 for AGP_Axial_Cells, which also had the lowest BMD, PRZ was inactive with HTPP, and further analysis was not performed with the ICE models. It should also be noted that PRZ was tested only with one cell type (U-2 OS) and it is not known if activity would have been seen with other cell lines.

ToxCast (Tier 2): The PRZ MOA involves activation of nuclear receptors and induction of liver enzymes as is seen with phenobarbital treatment in rodents (Braeuning et al., 2014; Elcombe et al., 2014; LeBaron et al., 2014). Acute exposure activates xenobiotic sensors (e.g., CAR, PPARα and PXR) (Angrish et al., 2016; LeBaron et al., 2014) that heterodimerize with RXR to bind at PXRE (Sugatani et al., 2004) or PPRE (Viswakarma et al., 2010; Wang & Negishi, 2003) to initiate expression of the CYPs and other proteins involved in lipophilic xenobiotic metabolism (Michalik et al., 2006). CYP4A10, CYP2B10 (CAR-associated), CYP1A1 (AhR-associated receptor) and CYP3A11 (PXR-associated) are the primary P450s involved in PRZ metabolism (LeBaron et al., 2014).

PRZ had active hit-calls for two Phase I and Phase II metabolic targets directly relevant to the MOA (e.g., human CYP1A1 and UDP-glucuronosyltransferase [UGT] induction in primary human liver cells) (LeBaron et al., 2014) (Table 5; Supplemental Tables 1 and 5). Other CYPs (primary human liver cells: CYP1A2, CYP2B6 and rat CYP2A1, human CYP2J2 and HepaRG CYP3A7) were also active with PRZ, but they are not associated with the known metabolic pathway. *In vitro* CYP activity with isolated primary human hepatocytes (CLD), or in cell-free (NVS) assays may occur because of a lack of interference by other *in vivo* processes. Although the PRZ Key Events begin with the activation of the nuclear receptors (CAR/PXR, PPARα, CAR, PXR), along with induction of CYPs (LeBaron et al., 2014). CAR, PXR, and PPARα were tested in three, eight and two ToxCast assays, respectively but they were either inactive (CAR and PPARα) or exceeded the cytotoxicity lower limit (PXR). Hence, the most significant molecular initiating events were not active, or not chemical-target specific in the ToxCast assays tested. The AED_{Human} for the CYP1A2 was 36 FD below the *in vivo* AdjLOEL, indicating low concordance but the other assays had FD ranging from 3.34 to 9.11 which was predictive with the PBTK model. The Z-Scores showed chemical-target specificity, although some of the CYPs are not directly related to the known MOA. Activity may be non-specific due to a lack of metabolic capabilities that would normally occur *in vivo*.

3.3.4. Carbaryl

The 3COMP model with CARB had the lowest FD between the AED_{Human} predictions compared to the *in vivo* AdjBMD using the HTTr, HTPP and ToxCast assay model inputs. The PBTK modeled AED_{Human} predicted FD were, generally about 250 % greater than those generated by the 3COMP model across the three assay types (Table 6; Supplemental Tables 1 and 5).

HTTr (Tier 1): CARB was tested in the three cell types (MCF-7, U-2 OS, HepaRG). HepaRG cells treated with CARB showed cholinergic transcriptomic signatures (100 genes in a transcriptomic signature) (Harrill et al., 2021) with a BMD of 4.64 μM. While this was not the lowest BPAC, it is directly associated with the MOA involving AChE inhibition (100 genes in a transcriptomic signature) (Harrill et al., 2021; US EPA, 2017)(Table 6; Supplemental Tables 1 and 5). The lowest BPAC was in MCF-7 cells for ETS1 transcription factor with a BMD of 0.60 μM (137 genes in a transcriptomic signature) (Harrill et al., 2021). ETS1 is associated with T-cell and other immune responses (Cauchy et al., 2016). Sterol regulatory element-binding factor (SREBF; BMD 0.95 μM; 21 genes in a transcriptomic signature) is associated with cholesterol biosynthesis (Yokoyama et al., 1993) and was activated in U-2 OS cells (Harrill et al., 2021). CARB exposure has not been shown to be associated with either cholesterol biosynthesis or immune response (US EPA, 2017). AED_{Human} for cholinergic response was + 1.85 FD above the *in vivo* AdjBMD, indicating the 3COMP produced highly concordant AED_{Human} PODs. However, CARB gene expression had the most potent endpoint with MCF-7 cells for ETS1 transcription factor, which is not associated with the main MOA for CARB.

HTPP (Tier 1): CARB was tested with U-2 OS cells only. DNA was the main target for PRZ in the HTPP assay (Table 6; Supplemental Tables 1 and 5). It was most active or had the lowest PAC with U-2 OS cells in the DNA "channel", with altered texture "module" in U-2 OS nuclei "compartment" (DNA_Texture_Nuclei; BMD: 15 μM; 15 features examined) (Table 6). This profile had an AED_{Human} of 45 FD above the *in vivo* AdjBMD with the 3COMP model, indicating low concordance. However, DNA in nuclei was identified as the main target.

ToxCast (Tier 2): AhR regulates CYP1A1 expression (Fallone et al. 2005) and the CYP3A, CYP1A and CYP2B families are activated through CAR/RXR and PXR/RXR with PXRE in the nuclear DNA (Ihunnah et al., 2011; Wang & Negishi, 2003). AhR (HepG2) and CYP1A1 (human primary hepatocytes) were both active identified in ToxCast, and are involved in the CARB metabolic pathway (Fallone et al. 2005). CYP2B6 and CYP1A2 (both in human primary hepatocytes) are also associated with CARB metabolic pathways (Tang et al., 2002). Human CYP19A1 is not a main CYP in CARB metabolism, but it may be active in ToxCast because it is a cell-free Novascreen assay that has no interference from whole cell processes. Three of the 5 CYP assays have AED_{Human} FD that are marginally greater than 10 FD above the *in vivo* AdjBMD with the 3COMP model indicating low concordance. The remaining 2/5 FD for CYPS had AED_{Human} less than 10 FD above the *in vivo* AdjBMD with the 3COMP model.

The AChE assay had an active hit-call with rat protein in a cell-free assay, which is directly associated with the main MOA. On the other hand, the Z-Score was below three, meaning that the target was not chemical specific and the AED_{Human} was 22 FD above the *in vivo* AdjBMD (low concordance). The assay was included in Table 6, however, since AChE inhibition is critical to CARB toxicity. AChE was tested in four cell-free Novascreen assays, including two performed with human protein, but they were either inactive, or greater than the cytotoxicity lower limit.

CARB was active in the developmental neurotoxicity rat cortical neuron cells with general neuronal activity (CCTE_Shafer_MEA_dev_firing_rate_mean_dn) and neural connectivity (CCTE_Shafer_MEA_dev_network_spike_number_dn) assays (Table 6). Both assays were in the down direction indicating a decrease in neural firing rate and neural connectivity that could occur during development. These effects support what is observed *in vivo* with AChE inhibition in brain leading to decreased neuro-muscular function and resulting in decreased motor activity, tremors, altered gait, decreased body temperature, decreased arousal, pinpoint pupils, increased salivation, and decreased grip strength, depending on dose (US EPA, 2017).

CARB had active hit-calls for increased percent metabolite change (STM_H9_OrnCyssISnorm_ratio_perc_up) or ratio of metabolite change (STM_H9_OrnCyssISnorm_ratio_dn) of CARB in human stem cells (Table 6; Supplemental Tables 1 and 5). The human H9 embryonic stem cell assay STM_H9_OrnCyssISnorm_ratio_dn measures a decrease in the ornithine (ORN) and cystine (CYSS) metabolite ratio secreted into the culture media, which is a biomarker for developmental toxicity (Zurlinden et al., 2020). The STM_H9_CystineISnorm_perc_up assay in human stem cells measures changes in cystine utilization which is also a biomarker for developmental toxicity. CARB has shown *in vivo* developmental effects but only at very high doses (92–136 mg/kg/day) (CDPR, 2014), where AChE inhibition occurs in brain at a BMD of 1.46 mg/kg/day in rodents, hence, neurotoxicity would occur before developmental effects (US EPA, 2017). All the assays described above had Z-Scores greater than three (Table 6; Supplemental Tables 1 and 5). The AED_{Human} was concordant with the *in vivo* AdjBMD at + 8.14 and + 8.70 FD.

3.4. Comparison of most concordant models in adults to Fetal PBTK modeled predictions

The most concordant ICE models for each chemical were compared to the Fetal PBTK model in Figs. 3-6 (Supplemental Tables 1 and 5) that covers gestation days 91 to 280. Note that the 3COMP and PBTK models had adult IVIVE modeled parameters. The *in vivo* regulatory ENDO, FIP and PRZ PODs were for adult animals, but the CARB POD was from rat pup data.

3.4.1. Comparison of Models: 3COMP in adults with PBTK Fetal

A graphed comparison was made between the FD values of the most concordant adult 3COMP or PBTK models and the FD of the Fetal PBTK model (Figs. 3-6; Supplemental Tables 1 and 5). The FD values shown in the Figures were rounded to the nearest whole number.

Endosulfan: The FD ratio between adult 3COMP and Fetal PBTK FD was approximately 1: 1.55 for each assay, with the FD for the fetal model always larger (raw data in Supplemental Tables 1 and 5). The most sensitive AED_{Human} predictions were with the Fetal PBTK model in the ToxCast acute neuroactivity neural connectivity category (-45 FD) and ToxCast acute neuroactivity bursting in the bursting category (–32 FD). In general, the Fetal PBTK FD were closer to one (i.e. $AED_{Human} \simeq$ *in vivo* AdjLOEL). There was little variability in FD between the models, that is, most FD were less than 10, indicating high concordance for both models (Fig. 3). The acute neurotoxicity assays were the most sensitive but least concordant compared to the other assays.

The FD ratio between the 3COMP and Fetal PBTK was low (1: 1.55 ratio), which meant that when a FD was above the AdjLOEL then the fetal FD was always higher, and the same if the FD was below the AdjLOEL. This could mean that the FD below the AdjLOEL were more health protective for fetuses by a 1: 1.55 ratio but not if the FD exceeded 10. This measurement is good for screening, but it could be further refined by use of known maternal and fetal pharmacokinetic and pharmacodynamic parameters if available (Kapraun et al., 2019; Pearce et al., 2017; Ring et al., 2017; Wambaugh et al., 2021).

Fipronil: The ratio between 3COMP and Fetal PBTK FD is about 1: 1.70 for each assay with the FD for the fetal model having larger FD (raw data in Supplemental Tables 1 and 5). While this is almost a twofold difference, the main concern is the FD below the AdjBMD. Based on these preliminary results, the model could be further refined to account for maternal/fetal variability during pregnancy (Kapraun et al., 2019; Pearce et al., 2017; Ring et al., 2017; Wambaugh et al., 2021).

The most sensitive AED_{Human} predictions were with the Fetal PBTK model in the ToxCast acute neuroactivity neural connectivity (-16 FD) and Phase II metabolism with a ToxCast sulfotransferase assay (-15 FD). There was little variability in FD between the models, that is, most FD were less than 5, indicating high concordance for both models (Fig. 4). The acute neurotoxicity assays and Phase II metabolism assays were the most sensitive and least concordant compared to the other assays. However, the FD with low concordance with less than or greater than 10 should be interpreted with the understanding that they are generally less reliable.

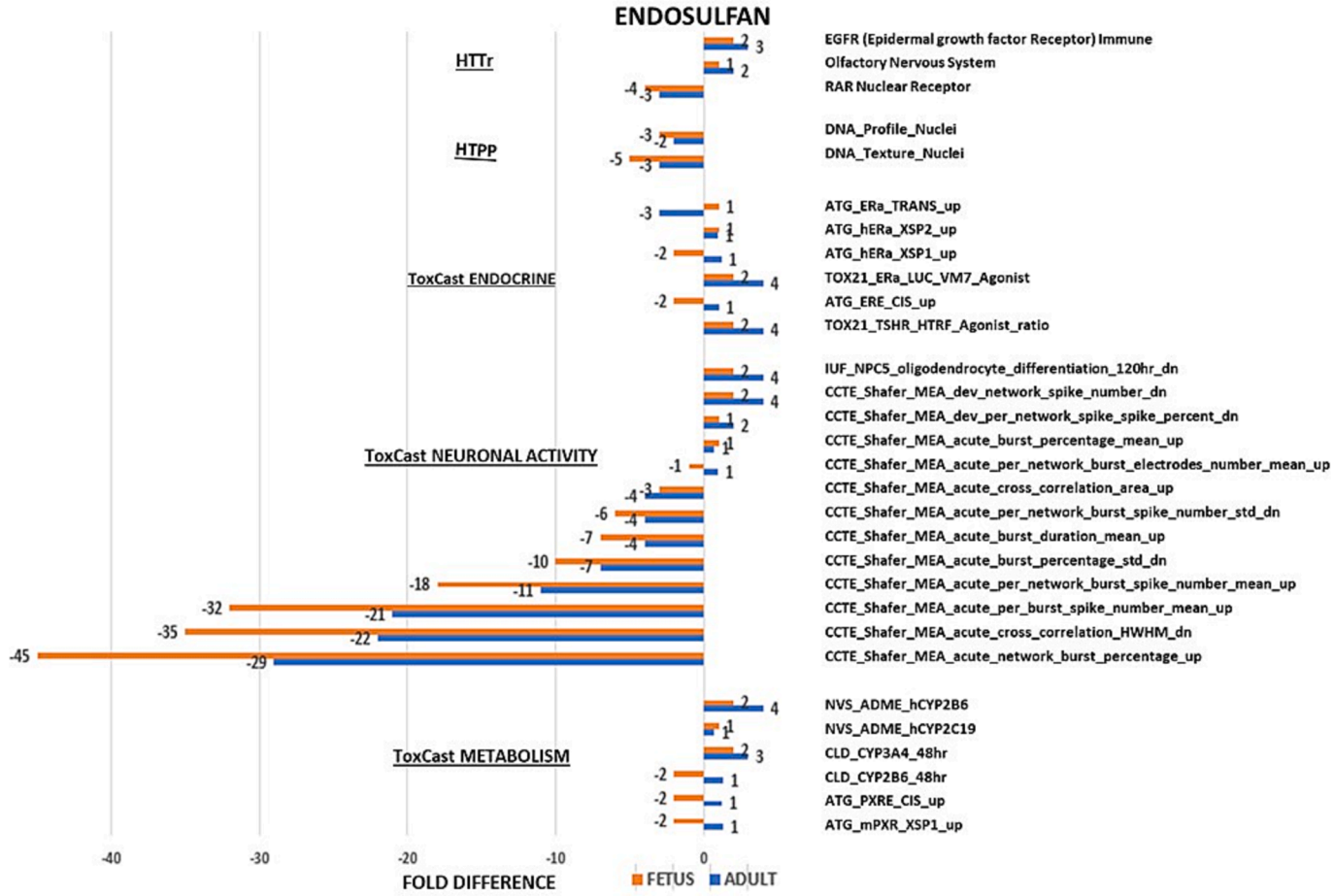

Fig. 3. Fold differences (FD) between AED_{Human} predictions for selected ENDO assays in the adult 3COMP and Fetal PBTK models and AdjLOEL *in vivo* regulatory POD. The assays are divided into HTTr, HTPP, and ToxCast (endocrine, neuronal activity, and metabolism). The FD are shown on each bar rounded to the nearest whole number.

Propyzamide: The ratio between 3COMP and Fetal PBTK FD is about 1: 1.14 (~equivocal) for each assay with the fetal model having the slightly larger FD (raw data in Supplemental Tables 1 and 5). The FD for PRZ were all below the *in vivo* AdjLOEL for the adult PBTK, and Fetal PBTK models (Fig. 5). The most sensitive AED_{Human} predictions were with the Fetal PBTK model for CYP P450 with HTTr (-47 FD) and ToxCast CYP1A2 (-41 FD). Since the FD for these targets in both the 3COMP and Fetal PBTK models have low concordance, they would need to be further refined to account for uncertainties. Overall, however, there was little variability in FD between the models, and most FD were less than 10, indicating generally, a high concordance for both models (Fig. 5).

Carbaryl: The ratio between 3COMP and Fetal PBTK FD is about 1: 2 for each assay with the FD for the fetal model having larger FD (raw data in Supplemental Tables 1 and 5). CARB FDs were all greater than one with both models (Fig. 6). The most sensitive but least concordant AED_{Human} were with the Fetal PBTK model for HTPP endpoint (DNA_Texture_Nuclei) at FD = 91 and HTTr cholinergic gene expression (Table 6 and Fig. 6). ToxCast CYP1A2 (29 FD). FD > 10 must be interpreted with caution since they may be less reliable. There was a 2-fold variability in FD between the models, that is, and most FD for adult 3COMP were greater than 5 (Fig. 6). The AChE inhibition assay had FD of greater than 10 for both models indicating low concordance with the major target for CARB. The developmental ToxCast assays in human embryonic stem cells measured changes in cystine utilization as a biomarker for developmental toxicity (Zurlinden et al., 2020). These assays had high concordance in the 3COMP but not the Fetal PBTK models. While CARB has shown *in vivo* developmental effects they are seen only at very high doses (92–136 mg/kg/day) (CDPR, 2014), hence, protecting for effects at lower doses would protect from developmental effects at higher doses.

3.5. *Assay Potency, concordance evaluations and Summary of fold differences for each assay Format*

In this study, assay potency is described as the threshold for perturbation of cellular biology (HTTr) (Harrill et al., 2021), category with the lowest Benchmark Dose (HTPP) (Nyffeler et al., 2020) and the lowest effective concentration leading to a 50 % change from control (AC_{50}) based on a best fit curve (ToxCast) (Filer, 2019; Filer et al., 2017; Harrill et al., 2018). The best fit curves are described on the CompTox Chemicals Dashboard for each chemical and assay after having gone through the tcpl (CompTox Chemicals Dashboard (epa.gov)). Table 7 shows the most potent assays for each assay method (i.e., HTTr, HTPP and ToxCast) and each chemical. The predicted AED_{Human} for the most potent assays is shown, along with the AdjLOEL/AdjBMD. Concordance was determined for relevance to MOA as well as for AED_{Human} PODs compared with regulatory Adj PODs (Table 7).

The Tier 1 HTTr assays did not reveal a lowest BPAC that is directly associated with ENDO, FIP or CARB toxicity. However, ENDO and PRZ had neurotoxicity-related gene expression signatures that could flag a potential for neurotoxicity even though the tested cells were not neurons. In addition PRZ activated a stress signature (DNA100) potentially associated with transcription for enzymes related to oxidative stress (catalase, D-amino acid oxidase, uric acid oxidase) and the MOA (LeBaron et al., 2014). The HTTr gene expression BMDs had the highest potency for PRZ and CARB, compared to HTPP (HTPP inactive with

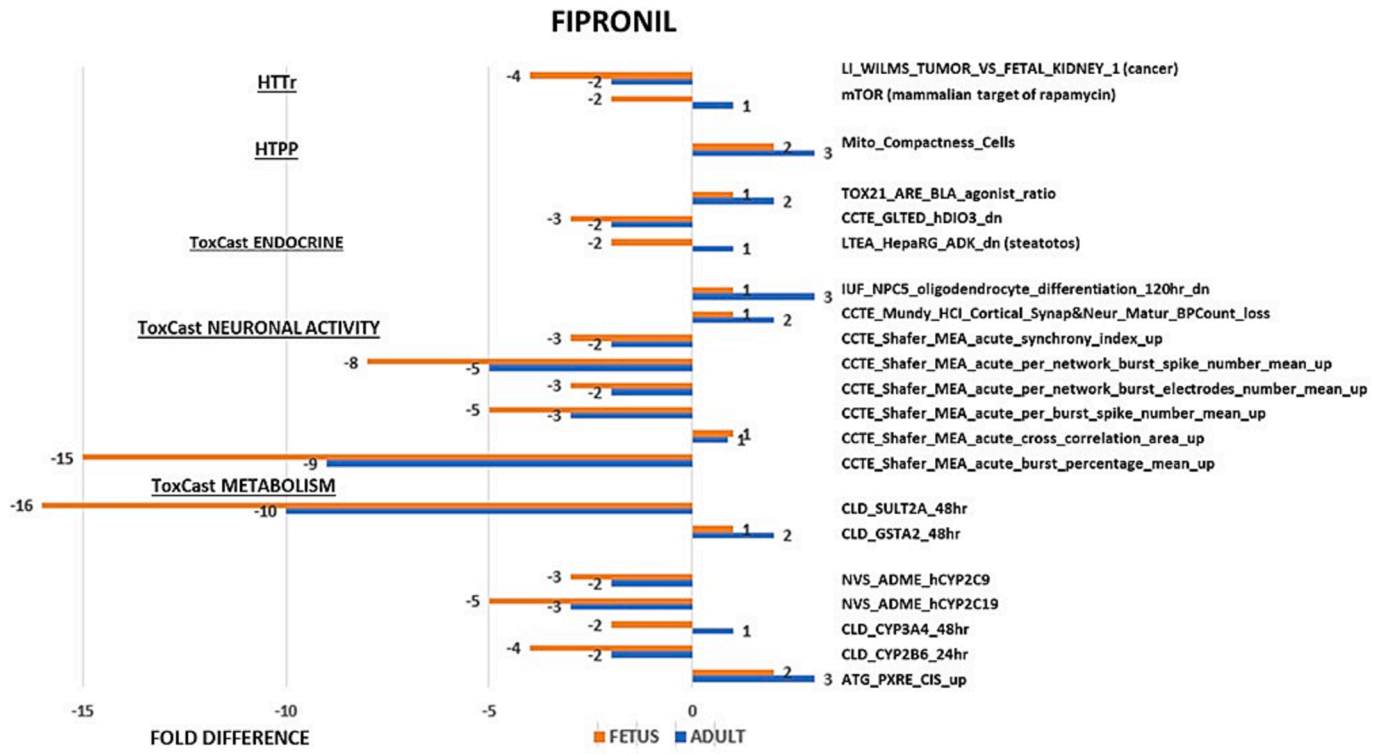

Fig. 4. Fold differences (FD) between AED_{Human} predictions for selected FIP assays in the adult 3COMP and Fetal PBTK models and AdjBMD *in vivo* regulatory POD. The assays are divided into HTTr, HTPP, and ToxCast (endocrine, neuronal activity, and metabolism). The FD are shown on each bar rounded to the nearest whole number.

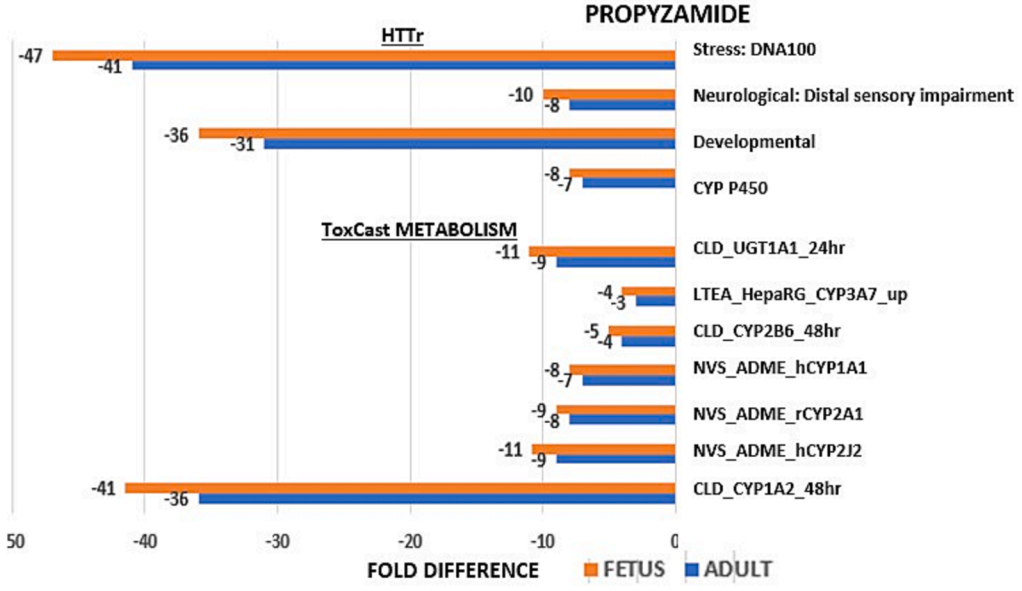

Fig. 5. Fold differences (FD) between AED_{Human} predictions for selected PRZ assays in the adult PBTK and Fetal PBTK models and AdjLOEL *in vivo* measured POD. The assays are divided into HTTr and ToxCast (metabolism). The FD are shown on each bar rounded to the nearest whole number.

PRZ) and ToxCast assays. HTTr AED_{Human} were highly concordant/concordant with the AdjLOEL/$AdjBMD_{10}$ for PRZ but for ENDO, FIP and CARB the results had low concordance.

The Tier 1 HTPP category-level endpoint that was most potently affected by ENDO and CARB was DNA texture in the nucleus. The HTPP BMDs were comparable to HTTr potency for ENDO, but not for CARB where the most potent HTPP BMD was > 25 times higher than what was seen for HTTr. DNA as a biological target was potentially concordant with what occurs *in vivo* based on the active nuclear receptor targets in ToxCast (i.e., PXRE for ENDO and AhR for CARB). HTPP PAC may be concordant for FIP where mitochondria were affected, however a direct association is unknown. PRZ was inactive in the HTPP assay. ENDO, FIP and PRZ HTPP AED_{Human} were concordant with the AdjLOEL/BMD_{10} where all FD were ≃2-3. Predicted CARB HTPP AED_{Human} was not concordant with the $AdjBMD_{10}$ (~45 FD) (Table 7).

Tier 2 ToxCast assay potency identified neurotoxicity pathways for

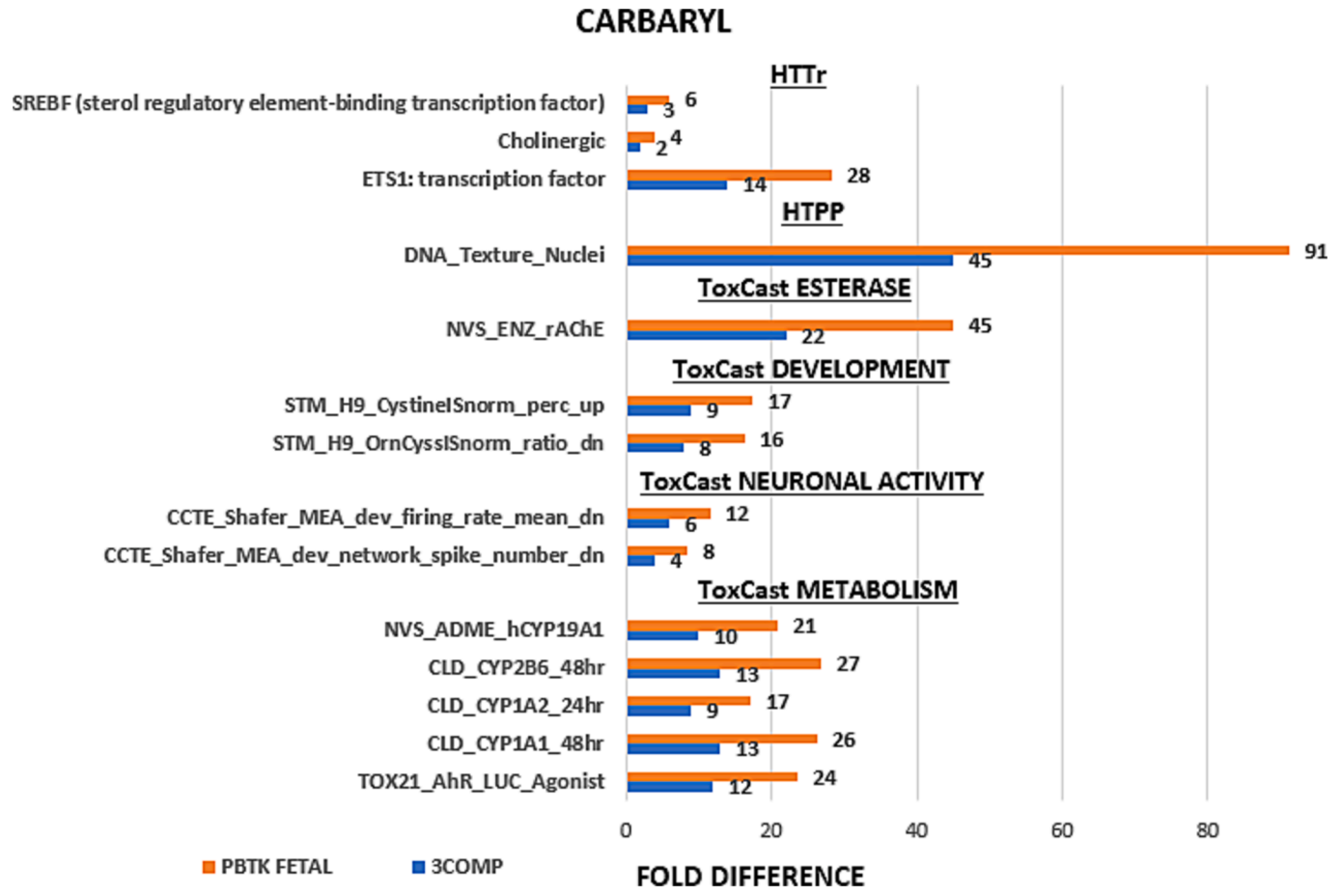

Fig. 6. Fold differences between AED_{Human} predictions for selected PRZ assays in the 3COMP or Fetal PBTK models and AdjBMD *in vivo* regulatory POD. The assays are divided into HTTr, HTPP, and ToxCast (esterase, development, neuronal activity, and metabolism). The FD are shown on each bar rounded to the nearest whole number.

the neurotoxic ENDO, FIP and CARB. Both ENDO and FIP, with similar MOAs, identified increased acute neuroactivity bursting patterns at or near the lowest AC_{50}s. CARB identified neuro-connectivity in a DNT assay as the lowest AC_{50}. However, since both ENDO and FIP act through the GABAa receptor, it is interesting that they were either tested in ToxCast with the wrong subunit (ENDO: subunit b3 on the GABAa receptor) or were not tested with GABA (FIP). PRZ showed the lowest AC_{50} for CYP1A2 which is not directly associated with the MOA but appears to be the most active in U-2 OS cells (LeBaron et al., 2014). ENDO had the lowest AC_{50} for a Phase II sulfotransferase enzyme which was equivocal with the AC_{50} for the neuroactivity assay (i.e., 0.19 vs. 0.21 μM). Overall, the ToxCast assays for each chemical were concordant with the MOA-associated toxicity and with the *in vivo* $AdjLOEL/BMD_{10}$ (Table 7).

Table 7 summarizes the AED_{Human} PODs with FD above, equivalent to and below the *in vivo* AdjPOD. Of most interest are the FDs that are within +/- 5 of the AdjLOEL/BMD. FD for ENDO had 48 % of AED_{Human} below, 41 % above and 11 % equivalent to the *in vivo* AdjPOD. Of the 29 total ENDO assays across the 3 test methods, there were 3/29 (all ToxCast) that had FD > 10 (low concordance) and the remainder FD ranged from −1.21 to + 6.64, indicating high concordance (FD ≤ 5) or concordance (>5 ≤ 10). FD for FIP had 62 % of AED_{Human} below, and 28 % above the *in vivo* AdjPOD. Of the 21 total FIP assays across the 3 test systems, the FD ranged from −1.37 to + 2.82, indicating high concordance. FD for PRO had 92 % of AED_{Human} below and 8 % above the *in vivo* AdjPOD. Of the 12 total PRO assays across the 3 test systems, there were 3/12 (2/4 HTTr; 1/7 ToxCast) that had FD > 10 (low concordance) and the remainder FD ranged from −3.34 to + 9.11, indicating high concordance (FD ≤ 5) or concordance (>5 ≤ 10). FD for CARB had 100 % AED_{Human} above the *in vivo* AdjPOD. Of the 14 total CARB assays across the 3 test systems, there were 6/14 (1/3 HTTr; 1/1 HTPP; 4/10 ToxCast) with FD > 10 (low concordance) and the remainder FD ranged from + 1.83 to + 8.70, indicating high concordance or concordance.

4. Discussion and conclusions

This case study provided a general workflow for how NAMs could be investigated for use in risk assessment as well as a predictive scope of various IVIVE models with the acutely neurotoxic pesticides described. The procedure involved the use of well-characterized pesticides so that the regulatory acute PODs, based on *in vivo* studies, could be compared to the predicted PODs, involving a progression of increasingly refined NAMs. Acute *in vivo* PODs were selected because the HTTr, HTPP and ToxCast *in vitro* assays were performed over acute periods (Harrill et al., 2021; Nyffeler et al., 2020; Williams et al., 2017). The pesticide MOAs are known for acute effects of ENDO, FIP and CARB, but the acute neurotoxic MOA for PRZ has not been specifically characterized (CDPR, 2008, 2023; US EPA, 2015, 2017). PRZ in rodent assays is mainly known for tumorigenesis through disruption of hypothalamus-pituitary-gonad/thyroid axes and from nuclear receptor/CYP induction leading to liver proliferation and hepatocarcinoma. However, it may be neurotoxic through oxidative stress (Corton et al., 2014; Sayre et al., 2008).

Pesticide risk assessment involves a thorough evaluation of the open literature, in addition to review of Health Effects Test Guideline studies, to provide the most health protective exposure levels (Overview of Risk Assessment in the Pesticide Program | US EPA) (US EPA, 1998). *In vitro* NAMs can produce similar values but they may, as was seen in several

Table 7
Assay potency, concordance evaluations and summary of fold differences for each assay format.

Assay Method	Assay	BMD/AC_{50} µM	AED_{Human} / AdjLOEL/AdjBMD (mg/kg)	Concordance: MOA/*in vivo* AdjPOD	Above/Equivalent/Below *in vivo* AdjPOD/Total Assay Selected[a]	FD Range[b]
Endosulfan						
HTTr	RAR Nuclear Receptor (HepaRG) Olfactory Nervous System (MCF-7 cells)	**BMD** 0.49 **BMD** 2.71	0.07/0.18 0.36/0.18	-/+ **Potential/+**	1/3 Below 2/3 Above	2.76 2.0 - 2.5
HTPP	DNA_Texture_Nuclei (U-2 OS Cells)	**BMD** 0.45	0.06/0.18	+/+	2/2 Below	2.18 – 3.0
ToxCast	CCTE_Shafer_MEA_acute_network_burst_percentage_up (Cortical neurons)	**AC_{50}** 0.047	0.01/0.18	+/+	3/24 Equivalent 11/24 Below 10/24 Above	1.0 – 1.06 1.21 – **29**[c] 1.18 - 3.79
Fipronil						
HTTr	LI_WILMS_TUMOR_VS_FETAL_KIDNEY_1 (Cancer; U-2 OS Cells)	**BMD** 0.82	0.11/0.25	-/+	2/2 Below	1.37 – 2.25
HTPP	Mito_Compactness_Cells (U-2 OS Cells)	**BMD** 4.96	0.067/0.25	?/+	1/1 Above	2.68
ToxCast	CLD_SULT2A_48hr (Primary human hepatocytes) CCTE_Shafer_MEA_acute_burst_percentage_mean_up (Cortical neurons)	**AC_{50}** 0.19 **AC_{50}** 0.21	0.03/0.25 0.03/0.25	+/+ +/+	11/18 Below 7/18 Above	1.16 - 10 1.16 – 2.82
Propyzamide						
HTTr	Stress: DNA100 (MCF7 Cells) Neurological: Distal sensory impairment (MCF-7 Cells)	**BMD** 0.38 **BMD** 1.85	0.05/4.0 0.23/4.0	+/+ **Potential/+**	4/4 Below	6.57 - **31**[c]
HTPP	No hit-calls >0.9	**Inactive**	Not applicable			
ToxCast	CLD_CYP1A2_48hr (Primary human hepatocytes)	**AC_{50}** 0.43	0.05/4.0	+/+	7/7 Below	3.34 - **36**[c]
Carbaryl						
HTTr	ETS1: transcription factor (MCF7 Cells)	**BMD** 0.60	2.06/0.146	-/-	3/3 Above	1.85 – **14**[c]
HTPP	DNA_Texture_Nuclei (U-2 OS Cells)	**BMD** 15	6.63/0.146	+/-	1/1 Above	**45**[c]
ToxCast	CCTE_Shafer_MEA_dev_network_spike_number_dn (cortical neurons)	**AC_{50}** 1.40	0.62/0.146	+/+	10/10 Above	4.23 – **22**[c]

Abbreviations: AC_{50}: concentration at 50% activity; AED_{Human}: administered equivalent dose in humans; BMD: benchmark dose; CCTE: assays performed with rat cortical neurons; 3COMP: 3 compartment IVIVE model; CYP: cytochrome P450; HepaRG: bi-potential hepatoma-derived cell line; HTPP: high throughput phenotypic profile; HTTr: high throughput transcriptomics; MCF7: human mammary adenocarcinoma cell line; RAR: retinoic acid receptor; TSHR: thyroid stimulating hormone receptor; U-2 OS: human osteosarcoma epithelial cell line.
a- FD below, equivalent to or above the *in vivo* AdjPOD out of the total number of assays selected.
b- Range of FD indicating high concordance (FD ≤5), concordance (>5≤10) and low concordance (FD >10) with the *in vivo* AdjLOEL/AdjBMD.
c-Red Text: There were few assays that had FD >10, as shown here: **1. ENDO:** ToxCast 3/18 >10 FD; **2. PRZ:** HTTr: 2/4 >10 FD; ToxCast 1/7 >10 FD; **3. CARB:** HTTr: 1/3 >10 FD; HTPP 1/1 >10 FD; ToxCast 4/10 >10 FD. For more detail see Tables 3 – 6.
d-The highest hit-call for HTPP was AGP_Axial_Cells at 0.65. The hit-call below the cutoff rendered the HTTP method inactive (data not reliable) for PRZ.
"+" indicates concordance; "-"indicates non-concordant with either the AED_{Human} or the AdjLOEL/AdjBMD, "?" unknown whether activity is related to the MOA/AOP; "Potential" indicates that gene expressions for neurotoxicity were detected at higher BMD than the most potent BMD, however since the cell types were not neurons, it is not known whether the results were incidental.
Green indicates FD above; Red indicates FD below and Yellow indicates FD equivalent to *in vivo* AdjLOEL/AdjBMD.

Abbreviations: AC_{50}: concentration at 50% activity; AED_{Human}: administered equivalent dose in humans; BMD: benchmark dose; CCTE: assays performed with rat cortical neurons; 3COMP: 3 compartment IVIVE model; CYP: cytochrome P450; HepaRG: bi-potential hepatoma-derived cell line; HTPP: high throughput phenotypic profile; HTTr: high throughput transcriptomics; MCF7: human mammary adenocarcinoma cell line; RAR: retinoic acid receptor; TSHR: thyroid stimulating hormone receptor; U-2 OS: human osteosarcoma epithelial cell line.
a- FD below, equivalent to or above the *in vivo* AdjPOD out of the total number of assays selected.
b- Range of FD indicating high concordance (FD ≤ 5), concordance (>5 ≤ 10) and low concordance (FD > 10) with the *in vivo* AdjLOEL/AdjBMD.
c-Red Text: There were few assays that had FD > 10, as shown here: **1. ENDO:** ToxCast 3/18 > 10 FD; **2. PRZ:** HTTr: 2/4 > 10 FD; ToxCast 1/7 > 10 FD; **3. CARB:** HTTr: 1/3 > 10 FD; HTPP 1/1 > 10 FD; ToxCast 4/10 > 10 FD. For more detail see Tables 3 – 6.
d-The highest hit-call for HTPP was AGP_Axial_Cells at 0.65. The hit-call below the cutoff rendered the HTTP method inactive (data not reliable) for PRZ.
"+" indicates concordance; "-"indicates non-concordant with either the AED_{Human} or the AdjLOEL/AdjBMD, "?" unknown whether activity is related to the MOA/AOP; "Potential" indicates that gene expressions for neurotoxicity were detected at higher BMD than the most potent BMD, however since the cell types were not neurons, it is not known whether the results were incidental.
Green indicates FD above; Red indicates FD below and Yellow indicates FD equivalent to *in vivo* AdjLOEL/AdjBMD.

examples, predict even lower values. This finding may mean that the dose at which a molecular initiating event occurs, especially if the target is related to a known MOA/AOP and associated with apical endpoints. This conclusion may be less certain when assays use cells that are not targeted by low chemical exposures such as may have occurred with all three test methods. Uncertainties involve a lack of *in vivo* complexity or metabolic capability such that when the FD are > 10 below or > 10 above the *in vivo* AdjPOD in non-target cells, the results may be difficult to interpret and need further analysis (Paul Friedman et al., 2020; Pearce et al., 2017). It cannot be concluded that AED_{Human} predictions of > 10 below the *in vivo* AdjLOEL/BMDs are more health protective because there are too many variables and unknowns, as well as data gaps in IVIVE models exist to predict with certainty. The open access databases and models mainly provide good screening and support for the *in vivo* presumptive MOA/AOPs.

While the three methods predicting AED_{Human} with ENDO generally had high concordance with what is seen *in vivo*, the GABAa receptor was inactive for reasons that perhaps had to do with the test design (Ratra et al., 2001). On the other hand, neurotoxicity was identified with HTTr, and ToxCast assays and notably, the neurotoxicity-related gene signature in HTTr was seen in MCF-7 non-neuronal cells. Tier 1 "screening" results showed neurotoxicity with HTTr and endpoints for nuclear DNA targets with HTPP in MCF-7 and U-2 OS cells, respectively. Endocrine targets were captured for ENDO with ToxCast (i.e., ERa and THSR: Table 3). *In vivo* ENDO affects reproduction and development but at doses higher than those for neurotoxicity (CDPR, 2008; Silva & Gammon, 2009). There were active DNT and neurodevelopment assays with ToxCast which are more closely associated with the MOA. For Tiers 1 and 2, the 3COMP model provided the lowest FD and the most highly concordant PODs with ENDO.

The FIP results for HTTr gene expression signatures in MCF-7 and U-2 OS cells and HTPP endpoints in U-2 OS cells were not associated with the known MOA, however it is interesting that the HTPP PAC was perturbation of the mitochondrial compactness in U-2 OS cells. Although FIP is associated with loss of spermatozoa mitochondrial membrane potential in rats (Khan et al., 2015) there is no direct association between mitochondrial compactness and changes in membrane potential. The cells used in Tier 1 were not neuronal and that may be the

reason why there were no MOA/AOP targets identified. Almost half of the ToxCast assays for FIP were associated with increased neuroactivity, as would occur *in vivo*, with the majority affecting neuro-connectivity. ToxCast identified Phase I and Phase II metabolic enzymes, kinases associated with steatosis and DNA binding associated with deiodinase which are all part of the FIP MOA. For Tiers 1 and 2, the 3COMP model provided the lowest FD and the most highly concordant PODs with FIP.

PRZ had HTTr signatures, such as CYP P450, neurological distal sensory impairment and stress DNA100 that could all be associated with the MOA. There was also a gene expression signature for developmental processes that may be incidental based on the lack of effects on such processes in the PRZ database (US EPA, 2015). HTPP was inactive with PRZ, but the assays were performed in U-2 OS cells that may not be the appropriate test cells to detect activity, since PRZ was active in HTTr and ToxCast. It is anticipated that HTPP will be tested in other cell types beyond U-2 OS to increase the number of chemicals with bioactivity that may also be active in ToxCast (Nyffeler et al., 2023). ToxCast captured the Phase I and Phase II metabolic processes for PRZ, which are relevant to the MOA. For Tiers 1 and 2, the PBTK model provided the lowest FD and the most highly concordant PODs with PRZ.

CARB HTTr captured the cholinergic signature in U-2 OS cells, which is directly associated with the MOA. HTPP endpoints indicate that CARB targets DNA as the most potent endpoint which can potentially be associated with nuclear receptor activity (Ahr) at a low AC_{50}. AChE was active with CARB in ToxCast, at an AC_{50} that was just below the cytotoxicity lower limit (7.37 vs. 7.47 μM), as were CYPS associated with the CARB metabolic pathway. Developmental neurotoxicity assays, showing decreased firing rates and decreased spike number comprised about 20 % of the total ToxCast assays. This is consistent with what has been seen with CARB as far as neuro-suppression (US EPA, 2017). For Tiers 1 and 2, the 3COMP model provided the lowest FD and the most highly concordant PODs with CARB.

While it can be argued that the cell types used for Tier 1 might not have the targeted pathways (e.g., MOA/AOP), like GABAa receptor subunits or neurons, and it is known (Harrill et al., 2021), or presumed (Nyffeler et al., 2023) that different gene expressions and morphological endpoints occur with different cell types, the current cell types used, have identified relevant targets. It would be interesting to see if future tests with neuronal cells show a greater level of potency, and better identify indicators of the MOA/AOPs than the current cell-types used in HTTr and in the HTPP assay reported on the CompTox Chemicals Dashboard.

Z-Scores were greater than or equal to three for all assays selected for further analysis. The test is meant to indicate a chemical target specificity. This is most likely true for the *in vitro* assays where there are not the full influences of *in vivo* processes. Hence, a positive Z-Score should be taken in context with what is known about a possible MOA, or AOP. The most concordant model, based on FD closest to one, was the 3COMP for all but PRZ, where the PBTK model provided better predictions. While the PBTK model has seven compartments, rather than only three, it may not be as concordant because there are insufficient TK parameters for model inputs for ENDO, FIP and CAR. This result suggests that model complexity did not necessarily provide better concordance. Moreover, interpretation of the predictiveness of modeled AED_{Human} values must consider several factors, including relevance of an assay to the MOA, availability of metabolic activation to generate a representative chemical-target interaction expressed as a transcriptomic signature, a phenotypic profile or an AC_{50}. Simply having a low FD is not enough to ensure an AED_{Human} is predictive.

The Fetal PBTK model was compared with the most predictive model where adult TK parameters were applied. The model has specific parameters for fetal growth and maternal changes throughout gestation (Kapraun et al., 2019). Fetal AED_{Human} FD were proportionately greater or lesser in a consistent ratio for each assay and chemical compared to those produced by the 3COMP or adult PBTK models (i.e., Ratio: Fetal FD: Adult FD, or Adult FD: Fetal FD). The proportion was consistent across all assays for a given chemical but was different for each chemical. This may be due to: 1) each assay for each chemical would have the same parameters for the model input; 2) because each chemical has TK parameters, the ratios would be different among chemicals; 3) the fetal and adult results are different because they encompass different physiological conditions. The fetal model also encompasses the maternal TK parameters, acknowledging that tissue volumes, blood flow rates, hematocrits, glomerular filtration rates and other parameters are constantly changing (Kapraun et al., 2019). This occurrence is especially notable for such targets as GABAa receptors because GABAa is primarily excitatory in early development and then it switches to inhibitory postnatally which would impact interpretation of results depending on the age of development (Kaila et al., 2014; Scheyer et al., 2020). Each output for the Fetal PBTK model represents a period beginning with 13 weeks of gestation at a time when data are more readily available. But the Fetal AED_{Human} output covers the entire term for an "average" mother and fetus. Instances where the Fetal PBTK FD were further below zero than the 3COMP or adult PBTK model, could be interpreted as increased toxicity to fetuses compared to adults during a specific window of susceptibility during gestation (Barton, 2005; Corley et al., 2003). On the other hand, as with the adult models, these findings should be interpreted with caution if the FDs are greater than 10. An advantage to this model is that it can be directly compared to adult IVIVE predictions based on the same assays, but future work could develop appropriate TK parameters for specific stages of development. All the FD for CARB were less than the AdjBMD *in vivo* value and the majority had high concordance or concordance.

This work offers a few indications of how NAMs can provide insights into gene expression signatures, morphological endpoints and more specific chemical targets that help support chemical characterization. The HTTr and HTPP are more recent additions to the CompTox Chemicals Dashboard, and they offer a broad initial screening to facilitate chemical prioritization based on bioactivity and potency. However, even if a Tier 1 assay is inactive, as was seen with PRZ in HTPP, tested only with U-2 OS cells, the absence of bioactivity does not mean that activity would not occur in a different cell type. If a chemical is inactive with several cell types over broad concentration ranges, then the weight of evidence could indicate that the chemical is likely inactive and may not present a human health hazard. In the future, as more cell types are used in the HTTr and HTPP tests, the hazard evaluations for many thousands of chemicals can be more thoroughly evaluated. The ToxCast Tier 2 methods provide a constantly expanding library of concentration response screens, that are supported by the tcpl, data flags, and robust curve-fitting algorithms developed by the US EPA and NTP (Filer et al., 2017; Thomas et al., 2019). It is acknowledged, however, that there is a real need to understand uncertainty and variability involved with the use of NAMs for regulatory decision-making (Watt & Judson, 2018). Development of pluripotent neuronal stem cells, such as those utilized in ToxCast developmental neurotoxicity assays (Shafer, 2021) can help evaluate the various responses that might occur among individuals with diverse genetic makeup. Improved metabolic capability in *in vitro* assays to represent chemical activation and target interaction more accurately, is a continuing process (Buckley et al., 2023). Machine learning/artificial intelligence methods are being incorporated into the NAMs to enhance predictive abilities, improve accuracy and efficiency in NAM development and data analysis (Buckley et al., 2023; Klambauer et al., 2023). This includes a continuing refinement of Maternal-Fetal PBTK models available through the open access ICE database (Kapraun et al., 2019). Open access is critical to making NAMs fit-for-purpose and user-friendly for regulatory agencies and research laboratories. It was stated succinctly in Buckley et al. (2023) "Considering the scale of chemical production, management requires transparent, systematic, timely, evidence-based decisions where computational approaches provide the only practical means of success." While it is undeniable that human and ecological diversity are complex and variable, technological advancements, including machine learning, open-access data availability and

method transparencies have provided substantial means for progress.

Funding

This research did not receive any specific grant from funding agencies in the public, commercial, or not-for-profit sectors.

Declaration of generative AI in scientific Writing

I have not used generative AI in my scientific writing.

Author contributions

I am the sole author and contributor to this article.

Declaration of competing interest

The authors declare that they have no known competing financial interests or personal relationships that could have appeared to influence the work reported in this paper.

Data availability

Data will be made available on request.

Acknowledgements

I would like to acknowledge Dr. Nisha Sipes, PhD, Assistant Center Director for Research Translations and Program/Regulatory Support at US EPA, Dr. Johanna Nyffeler, PhD, Center for Computational Toxicology and Exposure, Office of Research and Development, US EPA, and Dr. Joshua Harrill, PhD, Cellular and Molecular Toxicologist, in US EPA's National Center for Computational Toxicology and Dr. Eric Kwok, PhD, Senior Toxicologist, Department of Pesticide Regulation, California Environmental Protection Agency for help in interpreting the HTTr and HTPP data and the ICE IVIVE methods.

Appendix A. Supplementary data

Supplementary data to this article can be found online at https://doi.org/10.1016/j.crtox.2024.100156.

References

Abalis, I.M., Eldefrawi, M.E., Eldefrawi, A.T., 1986. Effects of insecticides on GABA-induced chloride influx into rat brain microsacs. J. Toxicol. Environ. Health 18 (1), 13–23. https://doi.org/10.1080/15287398609530844.

Abass, K., Turpeinen, M., Rautio, A., Hakkola, J., & Pelkonen, O. (2012). Metabolism of pesticides by human cytochrome P450 enzymes in vitro–a survey. *Insecticides—advances in integrated pest management*, 165-194.

Abedini, J., Cook, B., Bell, S.M., Chang, X., Choksi, N., Daniel, A.B., Hines, D., Karmaus, A.L., Mansouri, K., McAfee, E., Phillips, J., Rooney, J., Sprankle, C.S., Allen, D.G., Casey, W.M., Kleinstreuer, N., 2021. Application of new approach methodologies: ICE tools to support chemical evaluations. Comput. Toxicol. 20, 100184 https://doi.org/10.1016/j.comtox.2021.100184.

Andrus, A. K., & Hukkanen, R. R. (2011). Pronamide: Acute Neurotoxicity Study in F344/DuCrl Rats. *Toxicology & Environmental Research and Consulting, The Dow Chemical Company, Midland, MI., Study ID: 101164, Chemical Code #: 694 ID #: SBRA 260827 E; DPR Vol. Record #: 317-0133 273313 EPA Reg. #: 62719-394 SB 950 #: 98* (September 7, 2011).

Angrish, M.M., Kaiser, J.P., McQueen, C.A., Chorley, B.N., 2016. Tipping the Balance: Hepatotoxicity and the 4 Apical Key Events of Hepatic Steatosis. Toxicol. Sci. 150 (2), 261–268. https://doi.org/10.1093/toxsci/kfw018.

Anvar, Z., Acurzio, B., Roma, J., Cerrato, F., Verde, G., 2019. Origins of DNA methylation defects in Wilms tumors. Cancer Lett. 457, 119–128.

Banga, S., Patil, G.P., Taillie, C., 2002. Direct calculation of likelihood-based benchmark dose levels for quantitative responses. Environ. Ecol. Stat. 9, 295–315.

Barton, H.A., 2005. Computational pharmacokinetics during developmental windows of susceptibility. J. Toxic. Environ. Health A 68 (11–12), 889–900.

Baumann, N., Pham-Dinh, D., 2001. Biology of oligodendrocyte and myelin in the mammalian central nervous system. Physiol. Rev. 81 (2), 871–927.

Bebe, F.N., Panemangalore, M., 2003. Exposure to Low Doses of Endosulfan and Chlorpyrifos Modifies Endogenous Antioxidants in Tissues of Rats. J. Environ. Sci. Health B 38 (3), 349–363. https://doi.org/10.1081/PFC-120019901.

Bell, S.M., Abedini, J., Ceger, P., Chang, X., Cook, B., Karmaus, A.L., Lea, I., Mansouri, K., Phillips, J., McAfee, E., Rai, R., Rooney, J., Sprankle, C.S., Tandon, A., Allen, D.G., Casey, W.M., Kleinstreuer, N.C., 2020. An integrated chemical environment with tools for chemical safety testing. Toxicol. In Vitro 67, 104916. https://doi.org/10.1016/j.tiv.2020.104916.

Boison, D., Scheurer, L., Zumsteg, V., Rülicke, T., Litynski, P., Fowler, B., Brandner, S., Mohler, H., 2002. Neonatal hepatic steatosis by disruption of the adenosine kinase gene. Proc. Natl. Acad. Sci. 99 (10), 6985–6990.

Braeuning, A., Gavrilov, A., Brown, S., Wolf, C.R., Henderson, C.J., Schwarz, M., 2014. Phenobarbital-Mediated Tumor Promotion in Transgenic Mice with Humanized CAR and PXR. Toxicol. Sci. 140 (2), 259–270. https://doi.org/10.1093/toxsci/kfu099.

Bray, M.-A., Singh, S., Han, H., Davis, C.T., Borgeson, B., Hartland, C., Kost-Alimova, M., Gustafsdottir, S.M., Gibson, C.C., Carpenter, A.E., 2016. Cell Painting, a high-content image-based assay for morphological profiling using multiplexed fluorescent dyes. Nat. Protoc. 11 (9), 1757–1774. https://doi.org/10.1038/nprot.2016.105.

Breen, M., Ring, C.C., Kreutz, A., Goldsmith, M.-R., Wambaugh, J.F., 2021. High-throughput PBTK models for in vitro to in vivo extrapolation. Expert Opinion on Drug Metabolism & toxicology(just-accepted.

Buckley, T.J., Egeghy, P.P., Isaacs, K., Richard, A.M., Ring, C., Sayre, R.R., Sobus, J.R., Thomas, R.S., Ulrich, E.M., Wambaugh, J.F., Williams, A.J., 2023. Cutting-Edge Computational Chemical Exposure Research at the U.S. Environmental Protection Agency. Environ. Int. 108097 https://doi.org/10.1016/j.envint.2023.108097.

Caride, A., Lafuente, A., Cabaleiro, T., 2010. Endosulfan effects on pituitary hormone and both nitrosative and oxidative stress in pubertal male rats. Toxicol. Lett. 197 (2), 106–112. https://doi.org/10.1016/j.toxlet.2010.05.006.

Carrão, D.B., dos Reis Gomes, I.C., Barbosa Junior, F., de Oliveira, A.R.M., 2019. Evaluation of the enantioselective in vitro metabolism of the chiral pesticide fipronil employing a human model: Risk assessment through in vitro-in vivo correlation and prediction of toxicokinetic parameters. Food Chem. Toxicol. 123, 225–232. https://doi.org/10.1016/j.fct.2018.10.060.

Carstens, K.E., Carpenter, A.F., Martin, M.M., Harrill, J.A., Shafer, T.J., Paul-Friedman, K., 2022. Integrating Data From In Vitro New Approach Methodologies for Developmental Neurotoxicity. Toxicol. Sci. kfac018 https://doi.org/10.1093/toxsci/kfac018.

Casabar, R.C.T., Wallace, A.D., Hodgson, E., Rose, R.L., 2006. Metabolism of Endosulfan-α by Human Liver Microsomes and Its Utility as a Simultaneous in Vitro Probe for CYP2B6 and CYP3A4. Drug Metab. Dispos. 34 (10), 1779–1785. https://doi.org/10.1124/dmd.106.010199.

Casida, J.E., 1993. Insecticide action at the GABA-gated chloride channel: Recognition, progress, and prospects. Arch. Insect Biochem. Physiol. 22 (1–2), 13–23. https://doi.org/10.1002/arch.940220104.

Cauchy, P., Maqbool, M.A., Zacarias-Cabeza, J., Vanhille, L., Koch, F., Fenouil, R., Gut, M., Gut, I., Santana, M.A., Griffon, A., Imbert, J., Moraes-Cabé, C., Bories, J.C., Ferrier, P., Spicuglia, S., Andrau, J.C., 2016. Dynamic recruitment of Ets1 to both nucleosome-occupied and -depleted enhancer regions mediates a transcriptional program switch during early T-cell differentiation. Nucleic Acids Res. 44 (8), 3567–3585. https://doi.org/10.1093/nar/gkv1475.

CDPR. (2014). Carbaryl (1-naphthyl methylcarbamate): Occupational and Bystander Risk Characterization Document. *Medical Toxicology Branch, Department of Pesticide Regulation, California Environmental Protection Agency, Sacramento, CA, June 23, 2014*.

CDPR. (2008). Endosulfan Risk Characterization Document. *https://www.cdpr.ca.gov/docs/whs/active_ingredient/index.htm, Medical Toxicology and Worker Health and Safety Branches Department Of Pesticide Regulation California Environmental Protection Agency*.

CDPR. (2023). Fipronil Risk Characterization Document. *Human Health Assessment Branch, Department of Pesticide Regulation, California Environmental Protection Agency (EPA) office of environmental health hazard assessment, https://www.cdpr.ca.gov/docs/risk/rcd/fipronil_rcd.pdf*.

Chang, X., Tan, Y.M., Allen, D.G., Bell, S., Brown, P.C., Browning, L., Ceger, P., Gearhart, J.M., Hakkinen, P.J., Kabadi, S.V., Kleinstreuer, N.C., Lumen, A., Matheson, J., Paini, A., Pangburn, H.A., Petersen, E.J., Reinke, E.N., Ribeiro, A.J.S., Sipes, N.A., Mumtaz, M., 2022. IVIVE: Facilitating the Use of In Vitro Toxicity Data in Risk Assessment and Decision Making. Toxics 10 (5), 232. https://www.mdpi.com/2305-6304/10/5/232.

Cole, L.M., Casida, J.E., 1986. Polychlorocycloalkane insecticide-induced convulsions in mice in relation to disruption of the GABA-regulated chloride ionophore. Life Sci. 39 (20), 1855–1862. https://doi.org/10.1016/0024-3205(86)90295-X.

Cole, L.M., Nicholson, R.A., Casida, J.E., 1993. Action of phenylpyrazole insecticides at the GABA-gated chloride channel. Pestic. Biochem. Physiol. 46 (1), 47–54.

Corley, R.A., Mast, T.J., Carney, E.W., Rogers, J.M., Daston, G.P., 2003. Evaluation of physiologically based models of pregnancy and lactation for their application in children's health risk assessments. Crit. Rev. Toxicol. 33 (2), 137–211.

Corton, J.C., Cunningham, M.L., Hummer, B.T., Lau, C., Meek, B., Peters, J.M., Popp, J. A., Rhomberg, L., Seed, J., Klaunig, J.E., 2014. Mode of action framework analysis for receptor-mediated toxicity: The peroxisome proliferator-activated receptor alpha (PPAR α) as a case study. Crit. Rev. Toxicol. 44 (1), 1–49.

Dourson, M.L., Felter, S.P., Robinson, D.T., 1996. Evolution of science-based uncertainty factors in noncancer risk assessment. Regul. Toxicol. Pharm. 24 (2), 108–120.

Elcombe, C.R., Peffer, R.C., Wolf, D.C., Bailey, J., Bars, R., Bell, D., Cattley, R.C., Ferguson, S.S., Geter, D., Goetz, A., Goodman, J.I., Hester, S., Jacobs, A., Omiecinski, C.J., Schoeny, R., Xie, W., Lake, B.G., 2014. Mode of action and human relevance analysis for nuclear receptor-mediated liver toxicity: A case studywith

phenobarbital as amodel constitutive androstane receptor (CAR) activator. Crit. Rev. Toxicol. 44, 64–82.
Ferreira, M., De Oliveira, P.R., Denardi, S.E., Bechara, G.H., Mathias, M.I.C., 2012. Action of the chemical agent fipronil (active ingredient of acaricide Frontline®) on the liver of mice: An ultrastructural analysis. Microsc. Res. Tech. 75 (2), 197–205.
Ffrench-Constant, R.H., Mortlock, D.P., Shaffer, C.D., MacIntyre, R.J., Roush, R.T., 1991. Molecular cloning and transformation of cyclodiene resistance in Drosophila: an invertebrate gamma-aminobutyric acid subtype A receptor locus. Proc. Natl. Acad. Sci. 88 (16), 7209–7213.
Ffrench-Constant, R.H., Rocheleau, T.A., Steichen, J.C., Chalmers, A.E., 1993. A point mutation in a Drosophila GABA receptor confers insecticide resistance. Nature 363 (6428), 449–451.
Ffrench-Constant, R.H., Anthony, N., Aronstein, K., Rocheleau, T., Stilwell, G., 2000. Cyclodiene insecticide resistance: from molecular to population genetics. Annu. Rev. Entomol. 45, 449–466. https://doi.org/10.1146/annurev.ento.45.1.449.
Filer, D.L., Kothiya, P., Setzer, R.W., Judson, R., Martin, M.T., 2017. tcpl: the ToxCast pipeline for high-throughput screening data. Bioinformatics 33 (4), 618–620 https://doi.org/0.1093/bioinformatics/btw680.
Filer, D. L. (2019). *The new ToxCast analysis*.
Filipsson, A.F., Sand, S., Nilsson, J., Victorin, K., 2003. The Benchmark Dose Method—Review of Available Models, and Recommendations for Application in Health Risk Assessment. Crit. Rev. Toxicol. 33 (5), 505–542. https://doi.org/10.1080/10408440390242360.
Flockhart, D.A., 1995. Drug Interactions and the Cytochrome P450 System. Clin. Pharmacokinet. 29 (1), 45–52. https://doi.org/10.2165/00003088-199500291-00008.
Gant, D.B., Eldefrawi, M.E., Eldefrawi, A.T., 1987. Cyclodiene insecticides inhibit GABAA receptor-regulated chloride transport. Toxicol. Appl. Pharmacol. 88 (3), 313–321. https://doi.org/10.1016/0041-008X(87)90206-7.
Germain, P., Chanmbon, P., Eichele, G., Evans, R.M., Lazar, M.A., Leid, M., De Lera, A.R., Lotan, R., Mangelsdorf, D.J., Gronemeyer, H., 2006. International Union of Pharmacology. LX. Retinoic Acid Receptors. *Pharmacological Reviews* 58 (4), 712–725. https://doi.org/10.1124/pr.58.4.4.
Gustafsdottir, S.M., Ljosa, V., Sokolnicki, K.L., Anthony-Wilson, J., Walpita, D., Kemp, M. M., Petri-Seiler, K., Carrel, H.A., Golub, T.R., Schreiber, S.L., Clemons, P.A., Carpenter, A.E., Shamji, A.F., 2013. Multiplex Cytological Profiling Assay to Measure Diverse Cellular States. PLoS One 8 (12), e80999.
Gutiérrez-Vega, S., Armella, A., Mennickent, D., Loyola, M., Covarrubias, A., Ortega-Contreras, B., Escudero, C., Gonzalez, M., Alcalá, M., Ramos, M.D.P., Viana, M., Castro, E., Leiva, A., Guzmán-Gutiérrez, E., 2020. High levels of maternal total tri-iodothyronine, and low levels of fetal free L-thyroxine and total tri-iodothyronine, are associated with altered deiodinase expression and activity in placenta with gestational diabetes mellitus. PLoS One 15 (11), e0242743.
Hainzl, D., Cole, L.M., Casida, J.E., 1998. Mechanisms for Selective Toxicity of Fipronil Insecticide and Its Sulfone Metabolite and Desulfinyl Photoproduct. Chem. Res. Toxicol. 11 (12), 1529–1535. https://doi.org/10.1021/tx980157t.
Hansen, L.A., Kosberg, K.A., 2019. Ethics, efficacy, and decision-making in animal research. In: Animal Experimentation: Working towards a Paradigm Change. Brill, pp. 275–288.
Harrill, J.A., Freudenrich, T., Wallace, K.B., Ball, K., Shafer, T.J., Mundy, W.R., 2018. Testing for developmental neurotoxicity using a battery of in vitro assays for key cellular events in neurodevelopment. Toxicol. Appl. Pharmacol. 354, 24–39. https://doi.org/10.1016/j.taap.2018.04.001.
Harrill, J.A., Everett, L.J., Haggard, D.E., Sheffield, T., Bundy, J.L., Willis, C.M., Thomas, R.S., Shah, I., Judson, R.S., 2021. High-throughput transcriptomics platform for screening environmental chemicals. Toxicol. Sci. 181 (1), 68–89.
Harrill, J., Shah, I., Setzer, R.W., Haggard, D., Auerbach, S.S., Judson, R., Thomas, R.S., 2019. Considerations for strategic use of high-throughput transcriptomics chemical screening data in regulatory decisions. Current Opinion in Toxicology 15, 64–75. https://doi.org/10.1016/j.cotox.2019.05.004.
Hines, D.E., Bell, S., Chang, X., Mansouri, K., Allen, D., Kleinstreuer, N., 2022. Application of an Accessible Interface for Pharmacokinetic Modeling and In Vitro to In Vivo Extrapolation [Perspective]. Front. Pharmacol. 13 https://doi.org/10.3389/fphar.2022.864742.
Ihunnah, C.A., Jiang, M., Xie, W., 2011. Nuclear receptor PXR, transcriptional circuits and metabolic relevance. Biochim. Biophys. Acta (BBA) - Mol. Basis Dis. 1812 (8), 956–963. https://doi.org/10.1016/j.bbadis.2011.01.014.
Jeong, J.W., Kim, D., Choi, J., 2022. Application of ToxCast/Tox21 data for toxicity mechanism-based evaluation and prioritization of environmental chemicals: Perspective and limitations. Toxicol. In Vitro 84, 105451. https://doi.org/10.1016/j.tiv.2022.105451.
Judson, R., Kavlock, R.J., Setzer, R.W., Hubal, E.A.C., Martin, M.T., Knudsen, T.B., Houck, K.A., Thomas, R.S., Wetmore, B.A., Dix, D.J., 2011. Estimating toxicity-related biological pathway altering doses for high-throughput chemical risk assessment. Chem. Res. Toxicol. 24, 451–462. https://doi.org/10.1021/tx100428e.
Judson, R., Houck, K., Martin, M., Knudsen, T., Thomas, R.S., Sipes, N., Shah, I., Wambaugh, J., Crofton, K., 2014. In Vitro and Modelling Approaches to Risk Assessment from the U.S. Environmental Protection Agency ToxCast Programme. Basic Clin. Paharmacol. Toxicol. 115, 69–76.
Judson, R., Houck, K., Martin, M., Richard, A.M., Knudsen, T.B., Shah, I., Little, S., Wambaugh, J., Setzer, R.W., Kothya, P., Phuong, J., Filer, D., Smith, D., Reif, D., Rotroff, D., Kleinstreuer, N., Sipes, N.K., Xia, M., Huang, R., Thomas, R.S., 2016. Analysis of the Effects of Cell Stress and Cytotoxicity on In Vitro Assay Activity Across a Diverse Chemical and Assay Space. Toxicol. Sci. 152 (2), 323–339.
Kaila, K., Price, T.J., Payne, J.A., Puskarjov, M., Voipio, J., 2014. Cation-chloride cotransporters in neuronal development, plasticity and disease. Nat. Rev. Neurosci. 15 (10), 637–654. https://doi.org/10.1038/nrn3819.
Kamijima, M., Casida, J.E., 2000. Regional Modification of [3H] Ethynylbicycloorthobenzoate Binding in Mouse Brain GABAA Receptor by Endosulfan, Fipronil, and Avermectin B1a. Toxicol. Appl. Pharmacol. 163 (2), 188–194. https://doi.org/10.1006/taap.1999.8865.
Kapraun, D.F., Wambaugh, J.F., Setzer, R.W., Judson, R.S., 2019. Empirical models for anatomical and physiological changes in a human mother and fetus during pregnancy and gestation [Report]. PLoS One 14, e0215906.
Kapraun, D.F., Sfeir, M., Pearce, R.G., Davidson-Fritz, S.E., Lumen, A., Dallmann, A., Judson, R.S., Wambaugh, J.F., 2022. Evaluation of a rapid, generic human gestational dose model. Reprod. Toxicol. 113, 172–188.
Khan, S., Jan, M.H., Kumar, D., Telang, A.G., 2015. Firpronil induced spermotoxicity is associated with oxidative stress, DNA damage and apoptosis in male rats. Pestic. Biochem. Physiol. 124, 8–14. https://doi.org/10.1016/j.pestbp.2015.03.010.
Klambauer, G., Clevert, D.-A., Shah, I., Benfenati, E., & Tetko, I. V. (2023). Introduction to the Special Issue: AI Meets Toxicology. In (Vol. 36, pp. 1163-1167): ACS Publications.
Kleinstreuer, N.C., Ceger, P., Watt, E.D., Martin, M., Houck, K., Browne, P., Thomas, R.S., Casey, W.M., Dix, D.J., Allen, D.G., Sakamuru, S., Xia, M., Huang, R., Judson, R., 2017. Development and Validation of a Computational Model for Androgen Receptor Activity. Chem. Res. Toxicol. 30 (4), 946–964. https://doi.org/10.1021/acs.chemrestox.6b00347.
Knudsen, T., Fitzpatrick, S.C., Abrew, K., Birnbaum, L., Chappelle, A., Daston, G., Dolinoy, D., Elder, A., Euling, S., Faustman, E., Fedinick, K., Franzosa, J., Haggard, D., Haws, L., Kleinstreuer, N., Louis, G., Mendrick, D., Rudel, R.A., Saili, K. S., Zurlinden, T., 2021. FutureTox IV Workshop Summary: Predictive Toxicology for Healthy Children. Toxicol. Sci. https://doi.org/10.1093/toxsci/kfab013.
Lakshmana, M.K., Raju, T.R., 1994. Endosulfan induces small but significant changes in the levels of noradrenaline, dopamine and serotonin in the developing rat brain and deficits in the operant learning performance. Toxicology 91 (2), 139–150. https://doi.org/10.1016/0300-483X(94)90140-6.
Lawrence, L.J., Casida, J.E., 1984. Interactions of lindane, toxaphene and cyclodienes with brain-specific t-butylbicyclophosphorothionate receptor. Life Sci. 35 (2), 171–178. https://doi.org/10.1016/0024-3205(84)90136-X.
LeBaron, M.J., Rasoulpour, R.J., Gollapudi, B.B., Sura, R., Kan, H.L., Schisler, M.R., Pottenger, L.H., Papineni, S., Eisenbrandt, D.L., 2014. Characterization of Nuclear Receptor-Mediated Murine Hepatocarcinogenesis of the Herbicide Pronamide and Its Human Relevance. Toxicol. Sci. 142 (1), 74–92.
Li, A.A., Makris, S.L., Marty, M.S., Strauss, V., Gilbert, M., Blacker, A., Zorrilla, L.M., Coder, P.S., Hannas, B., Lordi, S., Schneider, S., 2019. Practical considerations for developmental thyroid toxicity assessments: What's working, what's not, and how can we do better? Regul. Toxicol. Pharm. https://doi.org/10.1016/j.yrtph.2019.04.010.
Lipton, J.O., Sahin, M., 2014. The neurology of mTOR. Neuron 84 (2), 275–291. https://doi.org/10.1016/j.neuron.2014.09.034.
Mazo, C., Lepousez, G., Nissant, A., Valley, M.T., Lledo, P.-M., 2016. GABAB receptors tune cortical feedback to the olfactory bulb. J. Neurosci. 36 (32), 8289–8304.
Mazzo, M., Balieira, K.V.B., Bizerra, P.F.V., Mingatto, F.E., 2018. Fipronil-induced decrease in the epididymal sperm count: oxidative effect and protection by vitamin E. Anim. Reprod. 15 (4), 1223–1230. https://doi.org/10.21451/1984-3143-ar2017-0040.
Michalik, L., Auwerx, J., Berger, J.P., Chatterjee, V.K., Glass, C.K., Gonzalez, F.J., Grimaldi, P.A., Kadowaki, T., Lazar, M.A., O'Rahilly, S., Palmer, C.N.A., Plutzky, J., Reddy, J.K., Spiegelman, B.M., Staels, B., Wahli, W., 2006. International Union of Pharmacology. LXI. Peroxisome Proliferator-Activated Receptors. Pharmacol. Rev. 58 (4), 726–741. https://doi.org/10.1124/pr.58.4.5.
Mohamed, F., Senarathna, L., Percy, A., Abeyewardene, M., Eaglesham, G., Cheng, R.N., Azher, S., Hittarage, A., Dissanayake, W., Sheriff, M.H.R., Davies, W., Buckley, N.A., Eddleston, M., 2004. Acute human self-poisoning with the N-phenylpyrazole insecticide fipronil–a GABAA-gated chloride channel blocker. J. Toxicol. Clin. Toxicol. 42 (7), 955–963. https://doi.org/10.1081/clt-200041784.
Moser, V.C., McDaniel, K.L., Phillips, P.M., Lowit, A.B., 2010. Time-Course, Dose-Response, and Age Comparative Sensitivity of N-Methyl Carbamates in Rats. Toxicol. Sci. 114 (1), 113–123. https://doi.org/10.1093/toxsci/kfp28.
Nyffeler, J., Willis, C., Lougee, R., Richard, A., Paul-Friedman, K., Harrill, J.A., 2020. Bioactivity screening of environmental chemicals using imaging-based high-throughput phenotypic profiling. Toxicol. Appl. Pharmacol. 389, 114876 https://doi.org/10.1016/j.taap.2019.114876.
Nyffeler, J., Haggard, D.E., Willis, C., Setzer, R.W., Judson, R., Paul-Friedman, K., Everett, L.J., Harrill, J.A., 2021. Comparison of Approaches for Determining Bioactivity Hits from High-Dimensional Profiling Data. SLAS Discovery 26 (2), 292–308. https://doi.org/10.1177/2472555220950245.
Nyffeler, J., Willis, C., Harris, F.R., Foster, M.J., Chambers, B., Culbreth, M., Brockway, R.E., Davidson-Fritz, S., Dawson, D., Shah, I., Paul-Friedman, K., Chang, D., Everett, L.J., Wambaugh, J.F., Patlewicz, G., Harrill, J.A., 2023. Application of Cell Painting for chemical hazard evaluation in support of screening-level chemical assessments. Toxicol. Appl. Pharmacol. 468, 116513 https://doi.org/10.1016/j.taap.2023.116513.
Ozoe, Y., Matsumura, F., 1986. Structural requirements for bridged bicyclic compounds acting on picrotoxinin receptor. J. Agric. Food Chem. 34 (1), 126–134. https://doi.org/10.1021/jf00067a035.
Paul Friedman, K., Gagne, M., Loo, L.H., Karamertzanis, P., Netzeva, T., Sobanski, T., Franzosa, J.A., Richard, A.M., Lougee, R.R., Gissi, A., Lee, J.J., Angrish, M., Dorne, J. L., Foster, S., Raffaele, K., Bahadori, T., Gwinn, M.R., Lambert, J., Whelan, M.,

Thomas, R.S., 2020. Utility of In Vitro Bioactivity as a Lower Bound Estimate of In Vivo Adverse Effect Levels and in Risk-Based Prioritization. Toxicol. Sci. 173 (1), 202–225. https://doi.org/10.1093/toxsci/kfz201.

Pavek, P., Dvorak, Z., 2008. Xenobiotic-Induced Transcriptional Regulation of Xenobiotic Metabolizing Enzymes of the Cytochrome P450 Superfamily in Human Extrahepatic Tissues. Curr. Drug Metab. 9, 129–143.

Pearce, R.G., Setzer, R.W., Strope, C.L., Sipes, N.S., Wambaugh, J.F., 2017. httk: R Package for High-Throughput Toxicokinetics. J. Stat. Softw. 79 (4), 1–26. https://doi.org/10.18637/jss.v079.i04.

Punt, A., Firman, J., Boobis, A.R., Cronin, M., Gosling, J.P., Wilks, M.F., Hepburn, P.A., Thiel, A., Fussell, K.C., 2020. Potential of ToxCast Data in the Safety Assessment of Food Chemicals. Toxicol. Sci. 174 (2), 326–340. https://doi.org/10.1093/toxsci/kfaa008.

Ratra, G.S., Kamita, S.G., Casida, J.E., 2001. Role of Human GABAA Receptor β3 Subunit in Insecticide Toxicity. Toxicol. Appl. Pharmacol. 172 (3), 233–240. https://doi.org/10.1006/taap.2001.9154.

Richard, A.M., Huang, R., Waidyanatha, S., Shinn, P., Collins, B.J., Thillainadarajah, I., Grulke, C.M., Williams, A.J., Lougee, R., Judson, R., 2020. The Tox21 10K compound library: collaborative chemistry advancing toxicology. Chem. Res. Toxicol. 34 (2), 189–216.

Ring, C.L., Pearce, R.G., Setzer, R.W., Wetmore, B.A., Wambaugh, J.F., 2017. Identifying populations sensitive to environmental chemicals by simulating toxicokinetic variability. Environ. Int. 106, 105–118.

Robinette, B.L., Harrill, J.A., Mundy, W.R., Shafer, T.J., 2011. In vitro assessment of developmental neurotoxicity: use of microelectrode arrays to measure functional changes in neuronal network ontogeny. Front. Neuroeng. 4, 1.

Roques, B.B., Lacroix, M.Z., Puel, S., Gayrard, V., Picard-Hagen, N., Jouanin, I., Perdu, E., Martin, P.G., Viguié, C., 2012. CYP450-Dependent Biotransformation of the Insecticide Fipronil into Fipronil Sulfone Can Mediate Fipronil-Induced Thyroid Disruption in Rats. Toxicol. Sci. 127 (1), 29–41. https://doi.org/10.1093/toxsci/kfs094.

Roques, B.B., Leghait, J., Lacroix, M.Z., Lasserre, F., Pineau, T., Viguié, C., Martin, P.G.P., 2013. The nuclear receptors pregnane X receptor and constitutive androstane receptor contribute to the impact of fipronil on hepatic gene expression linked to thyroid hormone metabolism. Biochem. Pharmacol. 86 (7), 997–1039. https://doi.org/10.1016/j.bcp.2013.08.012.

Sabatino, L., Vassalle, C., Del Seppia, C., Iervasi, G., 2021. Deiodinases and the Three Types of Thyroid Hormone Deiodination Reactions. Endocrinol Metab (seoul) 36 (5), 952–964. https://doi.org/10.3803/EnM.2021.1198.

Sasaki, T., Hiroki, K., Yamashita, Y., 2013. The role of epidermal growth factor receptor in cancer metastasis and microenvironment. Biomed Res. Int. 2013, 546318 https://doi.org/10.1155/2013/546318.

Sayre, L.M., Perry, G., Smith, M.A., 2008. Oxidative stress and neurotoxicity. Chem. Res. Toxicol. 21 (1), 172–188.

Schantz, S.L., Widholm, J.J., 2001. Cognitive effects of endocrine-disrupting chemicals in animals. Environ. Health Perspect. 109 (12), 1197–1206.

Scheyer, A.F., Borsoi, M., Wager-Miller, J., Pelissier-Alicot, A.-L., Murphy, M.N., Mackie, K., Manzoni, O.J.J., 2020. Cannabinoid exposure via lactation in rats disrupts perinatal programming of the gamma-aminobutyric acid trajectory and select early-life behaviors. Biol. Psychiatry 87 (7), 666–677.

Schmeisser, S., Miccoli, A., von Bergen, M., Berggren, E., Braeuning, A., Busch, W., Desaintes, C., Gourmelon, A., Grafström, R., Harrill, J., Hartung, T., Herzler, M., Kass, G.E.N., Kleinstreuer, N., Leist, M., Luijten, M., Marx-Stoelting, P., Poetz, O., van Ravenzwaay, B., Tralau, T., 2023. New approach methodologies in human regulatory toxicology – Not if, but how and when! Environ. Int. 178, 108082 https://doi.org/10.1016/j.envint.2023.108082.

Shafer, T.J., Brown, J.P., Lynch, B., Davila-Montero, S., Wallace, K.B., Paul-Friedman, K., 2019. Evaluation of Chemical Effects on Network Formation in Cortical Neurons Grown on Microelectrode Arrays. Toxicol. Sci. 169 (2), 436–455. https://doi.org/10.1093/toxsci/kfz052.

Shafer, T. J. (2021). Applying assays from the In Vitro Developmental Neurotoxicity Testing Battery to Compare DL- to L-Glufosinate Activity [Internet]. *https://doi.org/10.23645/epacomptox.17372606.v1*.

Shanks, N., Greek, R., Greek, J., 2009. Are animal models predictive for humans? Philos. Ethics Humanit. Med. 4, 2. https://doi.org/10.1186/1747-5341-4-2.

Sheffield, T., Brown, J.P., Davidson, S., Friedman, K.P., Judson, R., 2021. Tcplfit2: An R-language general purpose concentration-response modeling package. Bioinformatics.

Silva, M.H., Gammon, D., 2009. An assessment of the developmental, reproductive, and neurotoxicity of endosulfan. Birth Defects Res. B 86 (1), 1–28. https://doi.org/10.1002/bdrb.20183.

Silva, M.H., Pham, N., Lewis, C., Iyer, S., Kwok, E., Solomon, G., Zeise, L., 2015. A Comparison of ToxCast Test Results with In Vivo and Other In Vitro Endpoints for Neuro, Endocrine, and Developmental Toxicities: A Case Study Using Endosulfan and Methidathion. Birth Defects Research (part b) 104, 71–89.

Sipes, N.S., Martin, M.T., Reif, D.M., Kleinstreuer, N.C., Judson, R., Singh, A.V., Chandler, K.J., Dix, D.J., Kavlock, R.J., Knudsen, T.B., 2011. Predictive Models of Prenatal Developmental Toxicity from ToxCast High-Throughput Screening Data. Toxicol. Sci. 124 (1), 109–127. https://doi.org/10.1093/toxsci/kfr220.

Soto, A.M., Chung, K.L., Sonnenschein, C., 1994. The pesticides endosulfan, toxaphene, and dieldrin have estrogenic effects on human estrogen-sensitive cells. Environ. Health Perspect. 102 (4), 380–383.

Sugatani, J., Nishitani, S., Yamakawa, K., Yoshinari, K., Sueyoshi, T., Negishi, M., Miwa, M., 2004. Transcriptional Regulation of Human UGT1A1 Gene Expression: Activated Glucocorticoid Receptor Enhances constitutive Androstane Receptor/Pregnane X Receptor-Mediated UDP-Glucuronosyltransferase 1A1 Regulation with Glucocorticoid Receptor-Interacting Protein 1. Mol. Pharmacol. 67 (3), 845–855. https://doi.org/10.1124/mol.104.007161.

Sutherland, T. D., Horne, I., Weir, K. M., Russell, R. J., & Oakeshott, J. G. (2004). Toxicity and Residues of Endosulfan Isomers. In G. W. Ware (Ed.), *Rev Environ Contam Toxicol* (pp. 99-113). Springer New York. https://doi.org/10.1007/978-1-4419-9100-3_4.

Tang, J., Cao, Y., Rose, R.L., Hodgson, E., 2002. In vitro metabolism of carbaryl by human cytochrome P450 and its inhibition by chlorpyrifos. Chem. Biol. Interact. 141 (3), 229–241. https://doi.org/10.1016/S0009-2797(02)00074-1.

Tang, J., Amin Usmani, K., Hodgson, E., Rose, R.L., 2004. In vitro metabolism of fipronil by human and rat cytochrome P450 and its interactions with testosterone and diazepam. Chem. Biol. Interact. 147 (3), 319–329. https://doi.org/10.1016/j.cbi.2004.03.002.

Thomas, R.S., Allen, B.C., Nong, A., Yang, L., Bermudez, E., Clewell III, H.J., Andersen, M.E., 2007. A Method to Integrate Benchmark Dose Estimates with Genomic Data to Assess the Functional Effects of Chemical Exposure. Toxicol. Sci. 98 (1), 240–248. https://doi.org/10.1093/toxsci/kfm092.

Thomas, R.S., Bahadori, T., Buckley, T.J., Cowden, J., Deisenroth, C., Dionisio, K.I., Frithsen, J.B., Grulke, C.M., Gwinn, M.R., Harrill, J.A., 2019. The next generation blueprint of computational toxicology at the US Environmental Protection Agency. Toxicol. Sci. 169 (2), 317–332.

Tokunaga, C., Yoshino, K., Yonezawa, K., 2004. mTOR integrates amino acid- and energy-sensing pathways. Biochem. Biophys. Res. Commun. 313 (2), 443–446. https://doi.org/10.1016/j.bbrc.2003.07.019.

Unnikrishnan, A., Karmaus, A., Hull, V., Chang, X., Borrel, A., To, K., Daniel, A., Cooper, S., Phillips, J., & McAfee, E. (2023). Integrated Chemical Environment: An Advanced Platform Aiding NAM-Based Chemical Assessments.

US EPA. (2002b). A Review Of The Reference Dose and Reference Concentration Processes. *Retrieved from https://www.epa.gov/sites/production/files/2014-12/documents/rfd-final.pdf*(EPA/630/P-02/002F December 2002 Final Report).

US EPA. (2018). Strategic plan to promote the development and implementation of alternative test methods within the TSCA program. In: US EPA Washington, DC.

US EPA. (1998). *Health effect Test Guidelines (OPPS 870)*. (EPA 712-C-98-189). August, 1998: U.S. Environmental Protection Agency, Washington, DC Retrieved from http://www.regulations.gov/#!documentDetail;D=EPA-HQ-OPPT-2009-0156-0019.

US EPA. (2002a). Reregistration Eligibility Decision for Endosulfan. *Prevention, Pesticides and Toxic Substances (7101), U.S. Environmental Protection Agency, Washington, DC* (November, 2002).

US EPA. (2015). Pronamide. Human Health Risk Assessment for Registration Review and to Support New Section 3 Use on Leaf Lettuce (Revised). *(https://www.epa.gov/endocrine-disruption/endocrine-disruptor-screening-program-tier-1-screening-determinations-and; accessed 3-2020), DB Barcode: 0422207, 0410291; PC Code: 101701*.

US EPA. (2017). Carbaryl: Draft Human Health Risk Assessment in Support of Registration Review. *Office Of Chemical Safety and Pollution Prevention, United States Environmental Protection Agency Washington, D.C. 20460; Decision No.: 517387; March 30, 2017*.

US EPA. (2023). *CompTox Chemicals Dashboard* Retrieved from: https://comptox.epa.gov/dashboard/.

Viswakarma, N., Jia, Y., Bai, L., Vluggens, A., Borensztajn, J., Xu, J., & Reddy, J. K. (2010). Coactivators in PPAR-Regulated Gene Expression. *PPAR Research, 2010* (Article ID 250126), 1-21. https://doi.org/10.1155/2010/250126.

Wambaugh, J. F., Pearce, R., Ring, C., Honda, G., Sfeir, M., Davis, J., Sluka, J. P., Sipes, N., Wetmore, B. A., & Setzer, W. (2021). *httk: High-Throughput Toxicokinetics*.

Wang, H., Negishi, M., 2003. Transcriptional Regulation of Cytochrome P450 2B Genes by Nuclear Receptors. Curr. Drug Metab. 4 (6), 515–525. https://doi.org/10.2174/1389200033489262.

Watt, E.D., Judson, R., 2018. Uncertainty quantification in ToxCast high throughput screening. PLoS One 13 (7), e0196963–e. https://doi.org/10.1371/journal.pone.0196963.

WHO. (2014). Harmonization Project Document 11: Guidance Document on Evaluating and Expressing Uncertainty in Hazard Characterization. *WHO Document Production Services, World Health Organization, the International Labour Organization and the United Nations Environment Programme, Geneva, Switzerland, (https://www.who.int/ipcs/methods/harmonization/uncertainty_in_hazard_characterization.pdf accessed 3-2020)*.

WHO. (2017). Guidance document on evaluating and expressing uncertainty in hazard characterization. *World Health Organization, Geneva, Switzerland, https://apps.who.int/iris/bitstream/handle/10665/259858/9789241513548-eng.pdf;sequence=1#:~:text=GUIDANCE%20DOCUMENT%20ON%20EVALUATING%20AND%20EXPRESSING%20UNCERTAINTY%20IN,sponsorship%20of%20the%20World%20Health%20Organization%2C%20the%20International; accessed 3-2020)*, xxii + 159 pp.

Wilkinson, M.D., Dumontier, M., Aalbersberg, I.J., Appleton, G., Axton, M., Baak, A., Blomberg, N., Boiten, J.-W., da Silva Santos, L.B., Bourne, P.E., Bouwman, J., Brookes, A.J., Clark, T., Crosas, M., Dillo, I., Dumon, O., Edmunds, S., Evelo, C.T., Finkers, R., Mons, B., 2016. The FAIR Guiding Principles for scientific data management and stewardship. Sci. Data 3 (1), 160018. https://doi.org/10.1038/sdata.2016.18.

Williams, A.J., Grulke, C.M., Edwards, J., McEachran, A.D., Mansouri, K., Baker, N.C., Patlewicz, G., Shah, I., Wambaugh, J.F., Judson, R., Richard, A.M., 2017. The CompTox Chemistry Dashboard: a community data resource for environmental chemistry. J Cheminform 9 (61), 1–27. https://doi.org/10.1186/s13321-017-0247-6.

Woodruff, T.J., Rayasam, S.D.G., Axelrad, D.A., Koman, P.D., Chartres, N., Bennett, D.H., Birnbaum, L.S., Brown, P., Carignan, C.C., Cooper, C., Cranor, C.F., Diamond, M.L., Franjevic, S., Gartner, E.C., Hattis, D., Hauser, R., Heiger-Bernays, W., Joglekar, R., Lam, J., Zeise, L., 2023. A science-based agenda for health-protective chemical assessments and decisions: overview and consensus statement. Environ. Health 21 (S1). https://doi.org/10.1186/s12940-022-00930-3.

Yang, L., Allen, B.C., Thomas, R.S., 2007. BMDExpress: a software tool for the benchmark dose analyses of genomic data. BMC Genomics 8 (1), 387. https://doi.org/10.1186/1471-2164-8-387.

Yokoyama, C., Wang, X., Briggs, M.R., Admon, A., Wu, J., Hua, X., Goldstein, J.L., Brown, M.S., 1993. SREBP-1, a basic-helix-loop-helix-leucine zipper protein that controls transcription of the low density lipoprotein receptor gene. Cell 75 (1), 187–197. https://doi.org/10.1016/S0092-8674(05)80095-9.

Zurlinden, T.J., Saili, K.S., Rush, N., Kothiya, P., Judson, R.S., Houck, K.A., Hunter, E.S., Baker, N.C., Palmer, J.A., Thomas, R.S., Knudsen, T.B., 2020. Profiling the ToxCast Library With a Pluripotent Human (H9) Stem Cell Line-Based Biomarker Assay for Developmental Toxicity. Toxicol. Sci. 174 (2), 189–209. https://doi.org/10.1093/toxsci/kfaa014.